UC Riverside

UC Riverside Electronic Theses and Dissertations

Title

Understanding Asynchrony in Homogeneous Metacommunities

Permalink

https://escholarship.org/uc/item/83b1f0jn

Author

Hayes, Sean M.

Publication Date

2017

Copyright Information

This work is made available under the terms of a Creative Commons Attribution-ShareAlike License, availalbe at https://creativecommons.org/licenses/by-sa/4.0/

Peer reviewed|Thesis/dissertation

eScholarship.org Powered by the California Digital Library
University of California

UNIVERSITY OF CALIFORNIA
RIVERSIDE

Understanding Asynchrony in Homogeneous Metacommunities

A Dissertation submitted in partial satisfaction
of the requirements for the degree of

Doctor of Philosophy

in

Ecology, Evolution, and Organismal Biology

by

Sean Hayes

September 2017

Dissertation Committee:

Dr. Kurt E. Anderson, Chairperson
Dr. Matt Daugherty
Dr. Jeff Diez

Copyright by
Sean Hayes
2017

The Dissertation of Sean Hayes is approved:

_____

_____

_____

Committee Chairperson

University of California, Riverside

Acknowledgments

First, I would like to thank my adviser, Kurt Anderson, without whose support, guidance, and insight none of this would have been possible. I would also like to thank the rest of my dissertation committee, Jeff Diez and Matt Daugherty for taking the time to check my work and see this crazy thing through. I am also deeply indebted to the rest of the Anderson and Regan labs, including Helen Regan, Ashkaan Fahimipour, Heather Hulton VanTassel, Parsa Saffarinia, Matthew Green, Ryan Conway, Pamela Rueda Cediel, Erin Conlisk, and Serj Danielian, for constantly exposing me to new ideas, providing feedback at every stage of development of this dissertation, and listen to my endless and oftentimes rambling descriptions of my research.

I must also acknowledge my parents, Roger and Marianne Hayes, who originally instilled in me a passion for science and the importance of pursuing higher education, and perhaps most importantly the stubbornness to actually see all of this through. Finally, I most deeply thank Iohana Seserman for her unending faith, support, patience, and warmth, who together with her dog Cruise and her cats, Sponge and Lyra, kept me focused and sane enough to make it to the end. I am so glad you like me enough to put up with all this nonsense, because you mean the world to me.

For the love of wisdom.

ABSTRACT OF THE DISSERTATION

Understanding Asynchrony in Homogeneous Metacommunities

by

Sean Hayes

Doctor of Philosophy, Graduate Program in Ecology, Evolution, and Organismal Biology
University of California, Riverside, September 2017
Dr. Kurt E. Anderson, Chairperson

It has become increasingly clear that communities in nature are often not isolated systems, but instead interact with other communities via the movement of organisms ('dispersal'), forming metacommunities. The dynamics of these metacommunities can differ dramatically from what is expected from studying individual communities alone, enabling many new mechanisms for the persistence of species within communities. Central to these mechanisms is asynchrony: differences in the timing or quality of dynamics among communities. Asynchrony is often assumed to arise from environmental differences, however it is also possible for asynchrony to emerge from interactions between identical communities, a phenomenon known as pattern formation.

Here we explore the role of pattern formation in metacommunity dynamics by investigating the mechanisms which lead to asynchrony among identical communities. While it is well known in the literature that the number, magnitude, and distribution of dispersal connections within a metacommunity can influence asynchrony, we demonstrate that measures describing the local stability of the synchronized state can vary independently from these properties of dispersal and plays an important role in the emergence of asynchrony in metacommunities. We also demonstrate that not only the frequency of asynchrony but the types and qualities of asynchronous dynamics vary dramatically between spatial structures with the same amount and distribution of dispersal.

These findings illustrate the importance of understanding the effect of dispersal structure on the dynamical quality of asynchrony, however methods for this are limited. Thus we develop and analyze a simplified model which allows prediction of the asynchronous dynamics possible for a given dispersal structure, and the conditions promoting different dynamical regimes.

Finally, we consider how the structure of interactions between species within communities influence asynchrony. We find that communities which cannot persist in the absence of dispersal among communities are the most prone to asynchrony. The net result is a negative feedback between community persistence in isolation and persistence in the presence of dispersal, confounding predicted relationships between community properties and persistence ability derived from the study of isolated communities alone.

Contents

List of Figures

List of Tables

Chapter 1

Introduction

Historically, ecological communities have been studied primarily as isolated, self-contained systems of interacting species. In this context, the persistence of species has been found to depend on the structure and type of interactions among species within communities (May 1972; Pascual & Dunne 2006). However communities in nature are rarely truly isolated in nature due to the ubiquity of organism movement, or dispersal. Through dispersal, communities are often linked with others forming complex spatially-extended 'metacommunities' (Leibold *et al.* 2004). Within these metacommunities dispersal enables new mechanisms for species persistence and can alter the dynamics of communities dramatically from what is expected from studies of isolated communities. Thus communities in nature rely on both the careful balance of interactions among species to persist and the spatial persistence mechanisms enabled by dispersal. Building a deeper understanding of communities and the persistence of species within them therefore requires both further study of the as-yet poorly understood roles of dispersal and interactions between both spatial and local persistence mechanisms in community dynamics.

An important determinant of dispersal's role in community dynamics is the existence of differences between communities within a metacommunity. Extinction-prone species can recolonize from neighboring communities, but only if local extinctions occur at different times for populations from neighboring communities (Brown & Kodric-Brown

1977). Similarly, dispersal can reduce variability among populations if the timing of fluctuations in population abundance differ, particularly when the population minimum of one neighbor occurs at the same time as the population maximum of another (Maser *et al.* 2007). Following this, communities which are synchronized, exhibiting the same dynamics at the same time, derive no benefit from dispersal and ultimately function as a single large, isolated community. Asynchrony, or differences between communities either in the timing or quality of dynamics, is crucial for the beneficial mechanisms of metacommunity dynamics to function. Dispersal naturally homogenizes and synchronizes communities, however, which can lead to the loss of any beneficial effect on metacommunity dynamics.

Due to dispersal's homogenizing influence, a major component of understanding metacommunity dynamics is identifying the conditions under which asynchrony can be maintained even in the presence of dispersal. It is often assumed that, in nature, this asynchrony is maintained due to environmental heterogeneity, or the intrinsic differences in the environment of each habitat patch within a metacommunity (Cottenie 2005; Leibold *et al.* 2004). There are alternatives however; in particular movement among communities can create stable asynchronous patterns, a phenomenon known as pattern formation (Turing 1952). Even when communities are identical, dispersal among them creates the possibility for new equilibria which would not be stable in isolation, requiring either a net gain or loss of abundance through dispersal. While these equilibria would not be stable individually, if the gain and loss of abundance is balanced across the whole metacommunity it can be stable regionally. This phenomenon appears across a variety of fields, most commonly in the context of the Turing instability. In this case dispersal not only enables alternative asynchronous equilibria, but also destabilizes the synchronized state, making asynchrony inevitable. Asynchrony can also occur without a Turing instability, however (Liu *et al.* 2013; Wolfrum 2012). In this case, the metacommunity (or other complex system) can switch between each of its multiple possible equilibria depending on initial conditions or perturbations.

Pattern formation is a particularly important process in the maintenance of asyn-

chrony as it can cause differences in community dynamics across space even in the absence of environmental heterogeneity (Hastings 1993; Solé *et al.* 1992). Even when communities are in every respect identical, highly complex and spatially heterogeneous patterns of dynamics can emerge due to pattern formation. This creates significant challenges for understanding the dynamics of metacommunities in nature, as it becomes very challenging to determine whether a given pattern of asynchronous dynamics is the result of differences in the environment, a manifestation of pattern formation, or a combination of both mechanisms (Bascompte & Solé 1995). Disentangling the effects of these various mechanisms requires detailed study of the synchronization dynamics of homogeneous metacommunities, formed of identical communities, to understand the role of pattern formation in shaping metacommunity dynamics.

The ability of identical communities to maintain asynchrony via pattern formation has been shown to depend primarily on two properties of metacommunities: the structure of dispersal between community patches, and the structure of interactions within communities. Concerning the effect of the structure of dispersal, it is well known in both ecology and the broader study of complex networks that connectivity, the number of dispersal connections between patches, and dispersal rate, the relative strength of dispersal or coupling represented by each connection, play a major role in determining whether or not a system can synchronize (Holyoak & Lawler 1996; Hong *et al.* 2002; Paradis *et al.* 1999; Watts 1999). Specifically, higher dispersal rate and connectivity make asynchrony impossible and synchrony inevitable. More recently it has also been shown that the distribution of connections between communities can also play a significant role (Holland & Hastings 2008; Watts & Strogatz 1998). Synchronization is most likely when connections are distributed evenly among community locations, with asynchrony becoming more common as connections are randomized among them. Structure encompasses a great deal more than these measures, however, leaving many open questions regarding the effects of structure on synchronization (Arenas *et al.* 2008). In **Chapter 2** we investigate the role of these other structual properties in maintaining asynchrony, finding a great

deal of variation in asynchrony and metacommunity dynamics even among metacommunity structures with identical dispersal, connectivity, and distribution of connectivity. We follow this analysis in **Chapter 3** with the formulation and analysis of a model which predicts much of this variation and reveals greater mechanistic detail about the role of structure in asynchronous pattern formation.

The structure of interactions within communities also plays an important role in determining asynchrony, although this is much less well understood, particularly in ecology. While it is intuitive and easy to demonstrate that the dynamics within a community (or any component of a complex, coupled system) has a strong influence in the dynamics that emerge when these components are connected (Arenas *et al.* 2008; Barahona & Pecora 2002), the incredible range of dynamics possible across all types of ecological communities makes prediction and generalization difficult. Moreover, many challenges remain in linking the structure of interactions within communities to the dynamics they produce, though much progress has been made particularly in analyzing the structure of trophic interactions in food webs (Brose *et al.* 2006; McCann *et al.* 1998). These studies chiefly focus on how the structure of food webs determines the ability of a community's species to coexist in an isolated context, however. In **Chapter 4**, we reapply this work to a spatial context by considering how differences in the structure of food webs influence the ability of those food webs to sustain asynchrony in space.

Altogether, we aim to provide a deeper understanding of the mechanisms driving the persistence of species and dynamics of communities in space through our investigation of asynchrony among identical communities. Considering pattern formation as a source of asynchrony is critical for predicting the conditions in which communities can maintain asynchrony, and thus the action of potentially vital spatial persistence mechanisms, in nature.

Bibliography

Arenas, A., Dıaz-Guilera, A., Kurths, J., Moreno, Y. & Zhou, C. (2008). Synchronization in complex networks. *Physics Reports*, 469, 93–153.

Barahona, M. & Pecora, L. M. (2002). Synchronization in small-world systems. *Physical Review Letters*, 89, 054101.

Bascompte, J. & Solé, R. V. (1995). Rethinking complexity: modelling spatiotemporal dynamics in ecology. *Trends in Ecology & Evolution*, 10, 361–366.

Brose, U., Williams, R. J. & Martinez, N. D. (2006). Allometric scaling enhances stability in complex food webs. *Ecology Letters*, 9, 1228–1236.

Brown, J. H. & Kodric-Brown, A. (1977). Turnover rates in insular biogeography: effect of immigration on extinction. *Ecology*, 58, 445–449.

Cottenie, K. (2005). Integrating environmental and spatial processes in ecological community dynamics. *Ecology Letters*, 8, 1175–1182.

Hastings, A. (1993). Complex interactions between dispersal and dynamics: lessons from coupled logistic equations. *Ecology*, 1362–1372.

Holland, M. D. & Hastings, A. (2008). Strong effect of dispersal network structure on ecological dynamics. *Nature*, 456, 792–794.

Holyoak, M. & Lawler, S. P. (1996). Persistence of an extinction-prone predator-prey interaction through metapopulation dynamics. *Ecology*, 1867–1879.

Hong, H., Choi, M.-Y. & Kim, B. J. (2002). Synchronization on small-world networks. *Physical Review E*, 65, 026139.

Leibold, M. A., Holyoak, M., Mouquet, N., Amarasekare, P., Chase, J., Hoopes, M., *et al.* (2004). The metacommunity concept: a framework for multi-scale community ecology. *Ecology Letters*, 7, 601–613.

Liu, Q.-X., Doelman, A., Rottschäfer, V., Jager, M. de, Herman, P. M., Rietkerk, M. & Koppel, J. van de (2013). Phase separation explains a new class of self-organized

spatial patterns in ecological systems. *Proceedings of the National Academy of Sciences*, 110, 11905–11910.

Maser, G. L., Guichard, F. & McCann, K. S. (2007). Weak trophic interactions and the balance of enriched metacommunities. *Journal of Theoretical Biology*, 247, 337–345.

May, R. M. (1972). Will a large complex system be stable? *Nature*, 238, 413–414.

McCann, K. S., Hastings, A. & Huxel, G. R. (1998). Weak trophic interactions and the balance of nature. *Nature*, 395, 794–798.

Paradis, E., Baillie, S., Sutherland, W. & Gregory, R. (1999). Dispersal and spatial scale affect synchrony in spatial population dynamics. *Ecology Letters*, 2, 114–120.

Pascual, M. & Dunne, J. A. (2006). *Ecological networks: linking structure to dynamics in food webs*. Oxford University Press.

Solé, R. V., Valls, J. & Bascompte, J. (1992). Spiral waves, chaos and multiple attractors in lattice models of interacting populations. *Physics Letters A*, 166, 123–128.

Turing, A. M. (1952). The chemical basis of morphogenesis. *Philosophical Transactions of the Royal Society of London B: Biological Sciences*, 237, 37–72.

Watts, D. J. (1999). *Small worlds: the dynamics of networks between order and randomness*. Princeton university press.

Watts, D. J. & Strogatz, S. H. (1998). Collective dynamics of 'small-world'networks. *Nature*, 393, 440–442.

Wolfrum, M. (2012). The Turing bifurcation in network systems: Collective patterns and single differentiated nodes. *Physica D: Nonlinear Phenomena*, 241, 1351–1357.

Chapter 2

Beyond connectivity: how the structure of dispersal influences metacommunity dynamics

2.1 Introduction

Modern ecology has demonstrated that spatial processes play a major role in community dynamics. Spatially extended communities ('metacommunities') differ fundamentally from the classical conception of individual well-mixed communities (Leibold *et al.* 2004) as their component parts (patches) can exhibit differing dynamics ('asynchrony'), while still interacting through dispersing organisms. Asynchrony can include a range of dynamical differences depending on operational definition, from variation in the timing of otherwise identical community dynamics to dramatic shifts in equilibrium values or limit cycle amplitudes. Asynchronous dynamics have many dramatic effects on metacommunities, enabling the persistence of extinction-prone species through rescue effects (Brown & Kodric-Brown 1977), reducing population variability through averaging (Maser *et al.* 2007), and otherwise buffering the effects of perturbations (Buckling *et al.* 2000; Chesson & Huntly 1997) relative to isolated communities. As the key feature governing

the effects of space on community dynamics, understanding the conditions necessary for asynchrony to occur is a crucial goal of metacommunity ecology (Gouhier *et al.* 2010; Steiner *et al.* 2011), and has implications for conservation, reserve design, and biological control (Crooks & Sanjayan 2006; Murdoch *et al.* 2003). It has been well demonstrated that high dispersal tends to synchronize communities and thereby remove the effects of space from metacommunities (Hastings 1993; Koelle & Vandermeer 2005). However, the structure of dispersal connections ('spatial structure') between community patches determines the amount of dispersal necessary to synchronize a metacommunity (Arenas *et al.* 2008), playing a central although less understood role in governing metacommunity dynamics.

A complete theory on the dynamics of ecological communities therefore requires that the effect of spatial structure on metacommunity synchronization be fully described. Thus far it has been well established that synchronization is strongly influenced by the number of dispersal connections, or 'connectivity,' (Holyoak & Lawler 1996; Liebhold *et al.* 2004; Paradis *et al.* 1999) and the evenness of their distribution among patches, or the 'degree' of each patch (Gilarranz & Bascompte 2012; Holland & Hastings 2008; Watts & Strogatz 1998). As a result connectivity and related measures have been the focus in studies of structure and dynamics (Bunn *et al.* 2000; Marleau *et al.* 2014; Plitzko & Drossel 2015; Saunders *et al.* 1991; Taylor *et al.* 1993). However such measures remove information about the patterning of connections among communities such as how often communities share neighbors, form tightly interconnected neighborhoods, and how distant communities are from these neighborhoods (Arenas *et al.* 2008). The patterning of connections among communities also includes many properties that may be unintuitive but play an important role dynamically such as the spectral properties of the connectivity matrix (Barahona & Pecora 2002). Because these elements of structure are more challenging to measure and observe, they are often overlooked and as a result the role of the patterning of connections in metacommunity synchronization has not been well described. Moreover, overlooking these features risks confounding the effects of connectivity and the patterns of connections on synchronization. Identifying the unique contribution of

the patterning of connections among communities is therefore necessary to understand how spatial structure determines synchronization in metacommunities.

Here we demonstrate the unique effects of dispersal connection patterning on the tendency of metacommunities to synchronize, independent of connectivity or degree distribution. To accomplish this, we consider a set of 'regular' spatial structures with the same number of connections between each patch and a completely even distribution of these connections among patches. The set of regular spatial structures we consider are therefore perfectly equivalent in terms of measures of connectivity, specifically the total number of connections and the evenness of their distribution among communities. Nevertheless, alternative measures describing the pattern of connections, such as the frequency of clustering and topological distance between communities, do differ among these structures and have been shown to influence synchronization (Arenas *et al.* 2008; Barahona & Pecora 2002; Watts & Strogatz 1998). We further asses the role of the pattern of connections among communities in synchronization by comparing the dynamics of a simple metacommunity model on regular structures with equal connectivity but varying patterns of connection. We consider a simple case of community dynamics, a predator-prey model, to focus on the role of spatial processes. Furthermore, by holding parameter values equal across all patches we guarantee that each patch is identical to every other across all spatial structures, as each patch has the same number of dispersal connections and local dynamics. These metacommunities are therefore completely homogeneous and highly prone to synchrony.

We explore the role of the patterning of dispersal connections on synchronization by analyzing the reaction of these metacommunities with regular spatial structures to a range of asynchronous initial conditions, simulating a spatially heterogeneous perturbation. These tests reveal the tendency of individual structures to either synchronize or switch to asynchronous states following perturbation, highlighting the role of connectivity-independent structure. We further determine how asynchrony influences the dynamics of communities, particularly how well asynchrony stabilizes an unstable

predator-prey interaction at both the regional and local scales. Through this analysis we hope to further reveal the deeply complex relationship between spatial structure and community interactions, a topic of central importance for understanding metacommunity ecology and explaining the spatial dynamics observed in nature.

2.2 Methods

To simulate metacommunity dynamics we chose a Rosenzweig-MacArthur predator-prey model (Rosenzweig & MacArthur 1963) with dispersal:

$$\frac{dH_i}{d\tau} = rH_i(1 - \frac{H_i}{K}) - \frac{aP_iH_i}{b + H_i} + D\sum_{j=1}^{n} L_{ij}H_j \tag{2.1}$$

$$\frac{dP_i}{d\tau} = \frac{caP_iH_i}{b + H_i} - mP_i + D\sum_{j=1}^{n} L_{ij}P_j \tag{2.2}$$

where H_i and P_i are the prey and predator abundances respectively in patch i, K is the prey's carrying capacity, a is the predator's attack rate, b is the half-saturation coefficient of the predator's functional response, c is the conversion rate of consumed prey to predator offspring, m is predator mortality, D is dispersal rate (equal for both species). The matrix L_{ij} is a negative Laplacian describing the structure of dispersal between patches; an off-diagonal element L_{ij}, $(i \neq j)$ indicates the presence (1) or absence (0) of dispersal from patch j to patch i and a diagonal element L_{ii} is the negative sum of off-diagonal elements for column i, reflecting the total amount of emigration from patch i. In our networks, dispersal is always bi-directional ($L_{ij} = L_{ji}$)

To further simplify model analyses we employ a non-dimensional form of Eqns. 2.1 and 2.2 (Holland & Hastings 2008):

$$\frac{dh_i}{dt} = h_i(1 - \theta h_i) - \frac{p_ih_i}{1 + h_i} + \delta\sum_{j=1}^{n} L_{ij}h_j \tag{2.3}$$

$$\frac{dp_i}{dt} = \frac{\phi p_ih_i}{1 + h_i} - \eta p_i + \delta\sum_{j=1}^{n} L_{ij}p_j \tag{2.4}$$

This model retains the same dynamics, but is rescaled in terms of ratios of initial parameters. This reduces the number of parameters while highlighting the relationships which

drive dynamics. Time is re-scaled in terms of the prey instantaneous per-capita growth rate ($\tau = rt$). As a result, dynamics are determined exclusively by the predator-prey conversion rate relative to prey growth($\phi = ca/r$), prey self-regulation ($\theta = b/K$), predator mortality relative to prey growth ($\eta = m/r$), dispersal relative to prey growth ($\delta = D/r$), and spatial structure (L) which remains unchanged from the previous equations. To complete the substitution predator and prey abundances are rescaled ($h = H/b, p = aP/rb$). To focus on the effects of changing spatial structure, we constrained dynamics to parameter values analyzed in Holland & Hastings 2008 corresponding to high-amplitude oscillations ($\phi = 5, \theta = .3, \eta = 1$). In nature these dynamics would correspond to a highly extinction prone, unstable predator-prey pair, and are therefore ideal for observing the effect of spatial stabilizing mechanisms on species interactions. Similarly, a single value of dispersal was used ($\delta = .018$). Preliminary simulations showed little effect of dispersal beyond the expected trend of increasing asynchrony with lower dispersal. Thus we selected a relatively high level of dispersal where asynchrony is possible but not universal to emphasize the effects of structure on asynchrony.

Spatial Structure

We explore the effects of spatial properties on asynchrony and community dynamics by varying spatial structure L. Specifically, we isolate properties of spatial structure independent of connectivity by using only regular structures. These regular structures are all constructed with ten patches and four connections per patch, for which fifty-six distinct structures are possible. Thus connectivity and related measures do not vary among these structures. Other properties expected to play a role in synchronization do vary among these structures however, specifically mean path length and transitivity (Arenas *et al.* 2008). Path length is the shortest number of dispersal connections an organism must cross to get from one patch to another; one for directly connected patches, two for those which share a neighbor but no direct connection, etc. Mean path length is the average of path lengths between all patches, and reflecting how isolated patches are from

each other. Similarly, transitivity is the proportion of connected patches which share a neighbor to those which don't, measuring the tendency of patches within a structure to form tightly interconnected clusters. These measures were calculated for our networks using the igraph package in R (Csardi & Nepusz 2006).

We also characterize spatial structure using spectral theory, which utilize the eigenvalues (λ) and eigenvectors (ν) of the spatial structure matrix as a Laplacian matrix, $-L$. Specifically, the ratio of the largest eigenvalue to the smallest non-zero eigenvalue ($\frac{\lambda_{max}}{\lambda_2}$) can be used to determine the stability of a metacommunity's synchronized state (Barahona & Pecora 2002). This has been shown for any general model of coupled dynamics $\frac{dX_i}{dt} = F(X_i) - \delta \sum_{j=1}^{n} (-L_{ij}) H(X_j)$, where $F(X_i)$ is the change in X due to local processes in patch i, and $H(X_j)$ describes the effect of interaction with patch j. The synchronized state of this model is S, such that $X_i(t) = S(t)$ for all times t when all patches are synchronized. To determine the stability of this state, a small perturbation ξ is introduced (which is a vector with an element for each patch) and separated into the components of the eigenvectors of the Laplacian ν by solving the linear system $\xi = \sum_{i=1} \zeta_i \nu_i$. Then, the change in each eigenvector is given by $\nu_i(t) = \zeta_i e^{[F'(S(t)) - \delta\lambda_i H'(S(t))]t}$ where $F'(S(t))$ and $H'(S(t))$ are the Jacobian matrices describing the effects of local dynamics F and dispersal interactions H on S at time t.

Following this, the term $[F'(S(t)) - \delta\lambda_i H'(S(t))]$ is the master stability function, and if it is greater than zero at any time the ith eigenmode is unstable, as perturbations of the ith eigenvector will always increase over time. For synchrony to be stable across all eigenvectors, $[F'(s) - \delta\lambda_i H'(s)]$ must be less than zero for all λ_i, the range of which can be found from the maximum (λ_{max}) and smallest non-zero eigenvalue (λ_2). Due to the Laplacian's zero row-sum, the zero eigenvalue is associated with an eigenvector with all elements equal and corresponds to synchrony; thus change in this eigenvector is ignored. The greater the range of asynchronous eigenvalues is in terms of the ratio between λ_{max} and λ_2, the more likely at least one value falls in the range where $[F'(S(t)) - \delta\lambda_i H'(S(t))]$ is less than zero regardless of the exact model used (Barahona & Pecora

2002). While the ratio $\frac{\lambda_{max}}{\lambda_2}$ is commonly used in the literature, we use the inverse $\frac{\lambda_2}{\lambda_{max}}$ to characterize our structures, as this has a more linear distribution among the structures we consider. Following this we expect structures with smaller values of $\frac{\lambda_2}{\lambda_{max}}$ to be more prone to asynchronous dynamics.

Simulation Methods

We ran the model with each of the fifty-six regular network structures with ten patches and four connections per patch to determine their tendency for asynchrony and resulting dynamics. As a metacommunity that starts as synchronous will always remain synchronous, asynchrony was initially introduced through variation in initial population abundance. For structure, two hundred replicates of dynamics were simulated and analyzed. A range of randomly generated initial conditions were used to determine the relative frequency of synchrony and the range of asynchronous state possible for each structure. Variation in the initial distribution was introduced for each replicate by randomly selecting abundances from the uniform interval $[.9\hat{x}, 1.1\hat{x}]$, where $\hat{x}$ is the unstable fixed-point equilibrium density of species x: for prey (h), $\hat{h} = \eta/(\phi - \eta)$ and for predators (p), $\hat{p} = (1 + \hat{h})(1 - \theta\hat{h})$. Dynamics were simulated for 20000 time steps, by which point greater than 95% of simulations had reached equilibrium. Dynamics were simulated by solving the model system with the R implementation (library deSolve) of the FORTRAN Odepack solver lsoda (Soetaert *et al.* 2010).

For each simulation, we measured a number of characteristics of metacommunity dynamics, particularly those describing the ability of both species to persist. As there is only a single tightly-coupled predator-prey pair, oscillations and variability are highly correlated between both species allowing us to simplify analysis by focusing on one species for which we chose the prey. First we measured asynchrony in terms of correlations between patch dynamics (ρ_{ij}), measured by the Pearson product-moment correlation coefficient. Given the deterministic nature of our simulations we use a strict definition for synchrony, $\rho_{ij} = 1$, considering patches with any form of dynamical dif-

ferences to be asynchronous. Each structure was then characterized by the frequency of synchrony, the number of simulations that resulted in synchrony divided by the total.

Differences in equilibria were further characterized by grouping patches into synchronized 'clusters' (Holland & Hastings 2008) and characterized by the number of clusters present; synchronous states having one cluster, and purely asynchronous states having as many clusters as patches, or ten. Finally, we describe differences in the extinction risk of synchronous and asynchronous equilibria in terms of the variability of prey, measured by the coefficient of variation (standard deviation divided by the mean) in the final 2000 time steps of each simulation. This was done both for the total regional abundance of the metacommunity, which shows the effects of averaging in asynchronous states, and for the local abundances of patches to describe the appearance and stabilizing properties of dynamical heterogeneity.

Source code in R for all methods available at github.com/SMHayes/Beyond-connectivity.

2.3 Results

Frequency of asynchrony

We observed a substantial amount of variation in the frequency of synchrony among metacommunities with regular spatial structures. Differences in the frequency of synchrony and the utility of mean path length, transitivity, and the eigenratio $\frac{\lambda_2}{\lambda_{max}}$ in predicting them are summarized in Figure 2.1. Of these measures, the eigenratio $\frac{\lambda_2}{\lambda_{max}}$ appears to be the best individual predictor of a metacommunity structure's tendency to synchronize. We also find that within our regular networks these measures are strongly correlated with one another; $\rho(\frac{\lambda_2}{\lambda_{max}}$, Transitivity) = .795, $\rho(\frac{\lambda_2}{\lambda_{max}}$, Mean Path Length) = .834, and ρ(Transitivity, Mean Path Length) = .720. As a result, little additional variation is explained by regressing all measures (R^2 = .663) relative to the predictive power of $\frac{\lambda_2}{\lambda_{max}}$

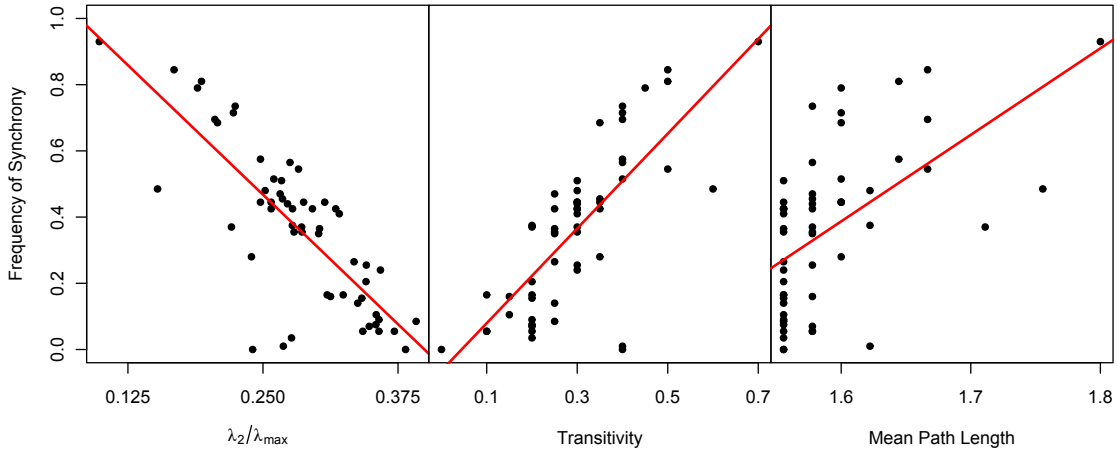

Effects	Model 1	Model 2	Model 3	Model 4
β_1 Eigenratio	-.797	-	-	-.636
β_2 Transitivity	-	.751	-	.369
β_3 Mean Path Length	-	-	.559	.183
Adjusted r^2	.628	.556	.300	.663

Figure 2.1: Predictive value of measures of spatial structure on metacommunity synchrony. Here, the frequency out of 160 simulations that resulted in synchronized dynamics are plotted against structural descriptors for each of 56 unique metacommunity structures. Standardized coefficients were obtained by fitting the full equation $Model\ 4\ (Frequency\ of\ Synchrony) = \beta_1(Eigenratio) + \beta_2(Transitivity) + \beta_3(Mean\ Path\ Length)$ and nested subsets using multiple linear regression as implemented using the lm command in the R package 'stats'. The associated adjusted r^2 values estimate how much variation in each metacommunity's frequency of synchrony is accounted for by the given measures of spatial structure. The eigenratio $\frac{\lambda_2}{\lambda_{max}}$ is the single best predictor of synchrony based on r^2 , being only slightly less accurate than the full model.

alone (R^2 = .628).

As expected, synchrony was very common among our metacommunities given the high degree of homogeneity inherent in regular spatial structures. Nevertheless, a number of spatial structures were highly resistant to synchronization, and in general the tendency toward synchrony varied considerably among structures. This presents a clear demonstration that the spatial variation among these networks plays a significant role in their dynamics despite no differences in connectivity both at the level of the entire structure and between individual patches. While the eigenratio $\frac{\lambda_2}{\lambda_{max}}$ appears to capture much of the dynamically relevant variation, a great deal remains unexplained even when mean path length and transitivity are included.

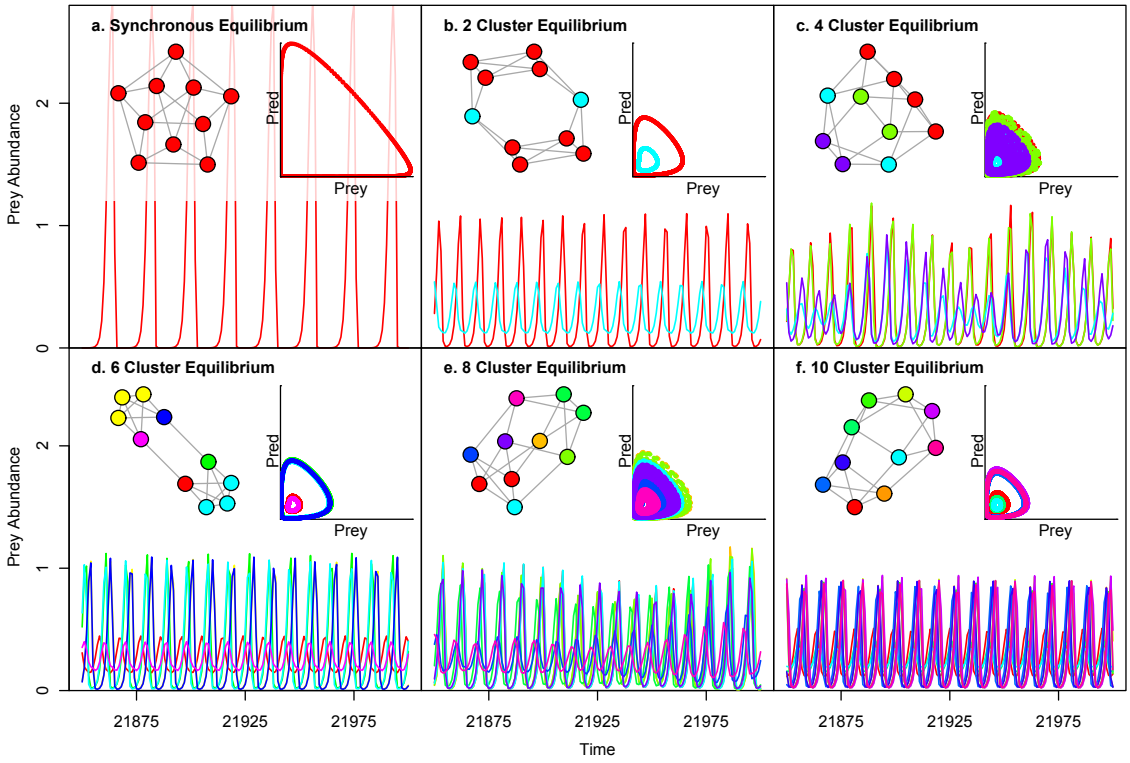

Figure 2.2: Examples of the different classes of dynamical behavior observed in our simulations, where patches with the same colors exhibit identical dynamics. While the dynamics of synchronized metacommunities (a.) are identical among all examples of their class at equilibrium, metacommunities with asynchronous equilibria (b.-f.) vary widely both in their dynamics and pattern of spatial clustering.

Asynchronous dynamics

Despite the strict homogeneity of our metacommunities, as each community is identical and connected to exactly four other communities, we observe a substantial range of different types of stable asynchronous dynamics, in which patches differentiate into several different internally synchronized dynamical regimes ('clusters'). We illustrate several examples of these dynamics in Figure 2.2 and compare them with the synchronous equilibrium (a) which is identical for all structures. Synchronous dynamics are characterized by extremely high-amplitude oscillations and significant periods of low abundance for both species. Unsurprisingly, asynchronous dynamics have universally lower variability than the synchronous state. Additionally, asynchronous dynamics

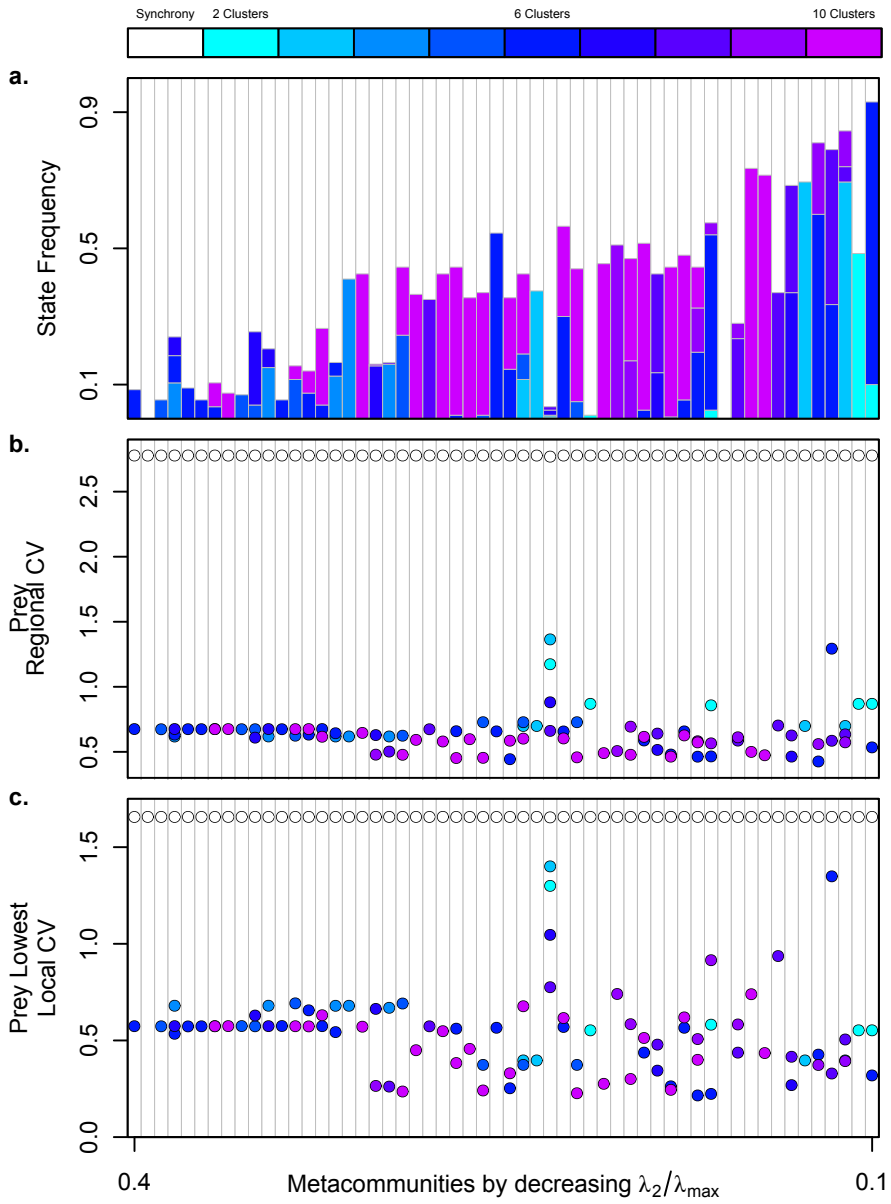

Figure 2.3: Illustration of the dynamical variation observed as a result of variation in metacommunity spatial structure and initial conditions. The y-axis shows each metacommunity structure ranked by decreasing eigenratio. In (a.) we show differences in the frequency of all observed spatial patterns of asynchrony, noting that many structures produce multiple types of stable spatial patterns. In (b.) and (c.) we show the effect of these various spatial patterns on the total regional and lowest observed local variability of the prey species calculated at the final 2000 time steps of each simulation. The completely synchronized state is always more variable than partially synchronized states, yet the degree to which variability is reduced due to asynchrony varies depending on the spatial structure of a given metacommunity, the pattern of clustering, and whether the local or regional scale is considered.

typically feature at least one synchronized cluster with oscillations of much higher average abundance and lower amplitude than the metacommunity average. These patches in many cases are phase-locked and adjacent to several high-amplitude patches (Fig. 2.2 b, d, e). In these cases their maxima can be seen to occur just before the maxima of high-amplitude patches, when abundances of high amplitude patches are very low. Dispersal is therefore having a relatively strong net negative effect on the low amplitude patches during their maxima, as migrants are sent to the high-amplitude patches at their minima at a much higher rate than they are received. This trend then switches following the low-amplitude patches' maxima, with dispersal having a net positive effect as the high amplitude patches increase toward their maxima. Asynchronous patterns can also be more complex, exhibiting complex multi-point limit cycles (Fig. 2.2 c) and secondary low-frequency oscillations (Fig. 2.2 e).

A full summary of the frequency and variability of asynchronous dynamics produced by each regular spatial structure is presented in Figure 2.3. The variability of predator-prey oscillations are universally lower for asynchronous equilibrium at both the local scale (Coefficient of variation of prey $.22 - 1.40$ for asynchrony, 1.66 for synchrony) and regional scale (Coefficient of variation of prey $.43 - 1.36$ for asynchrony, 2.78 for synchrony). While this is expected, the degree to which asynchronous equilibrium states vary relative to each other is surprising. Additionally, we note that different asynchronous equilibria vary in their effect on the regional and local scales. Specifically, states with two to three clusters typically have higher regional variability (Fig. 2.3b) than higher clusters states, but many have patches with equal or lower local variability (Fig. 2.3c). This suggests that the variability of asynchronous states is being influenced by multiple mechanisms acting at different spatial scales, and the degree to which each mechanism plays a role varies depending on structure and pattern of clustering.

Any given spatial structure may produce multiple types of asynchronous patterns with varying numbers of synchronized clusters (Figure 2.3). This leads, somewhat surprisingly, to considerable differences in the pattern of asynchrony and predator-prey

dynamics produced even by the same dispersal structure. While a single structure may produce multiple types of dynamics, each asynchronous regime is tied to a specific pattern of clusters. The patterns possible are constrained by the structure of dispersal, specifically in that all patches belonging to a synchronized cluster are connected to the same types and numbers of patches belonging to other synchronized clusters. For example, in the case of Figure 2.2b, teal patches are always connected to four red patches, and red patches to three red patches and one teal patch. This guarantees that patches which are synchronized experience the same fluctuations as a result of dispersal. Thus, the structure of dispersal connections within the metacommunity is influencing not only the frequency of asynchrony, but also the variability of asynchronous dynamics by constraining how partially synchronized clusters can be distributed.

Altogether it is extremely challenging to predict the variation in asynchronous dynamics we observe from spatial structure alone. In Figure 2.3a it is clear that although the total frequency of asynchronous dynamics decrease with the eigenratio of the structure, the number of clusters observed in these patterns is highest at intermediate levels. Because lower cluster states often have higher regional variability this means that patches with intermediate values of the eigenratio also have the lowest regional variability. This does not hold for local variability, however. Furthermore, the actual variability of each structure will vary dramatically depending on the specific pattern of clustering realized.

2.4 Discussion

Our results demonstrate that the tendency of metacommunities to synchronize is strongly influenced by the pattern of connections among community patches, even when connectivity and degree distribution are held constant. This is an important step to better understanding how metacommunity dynamics are influenced by spatial structure given the focus on connectivity in the literature (Bunn *et al.* 2000; Marleau *et al.* 2014; Plitzko & Drossel 2015; Saunders *et al.* 1991; Taylor *et al.* 1993). We further illustrate that differ-

ences in the pattern of connections and initial conditions among communities lead to the emergence of a wide array of stable asynchronous dynamics, leading to substantial differences in the potential persistence of an unstable predator-prey interaction at both the regional metacommunity and local patch level, despite the otherwise strict homogeneity of our metacommunities in which each community is identical and connected to exactly four other community patches. Our study is the first to produce this range of dynamical variation as a result of such subtle changes in spatial structure; this contrasts with earlier work that has only produced comparable variation through heterogeneity in connectivity or degree distribution (Gilarranz & Bascompte 2012; Holland & Hastings 2008), differences in dispersal among species (de Roos *et al.* 1998), or alteration of community dynamics in more complex models (Hata *et al.* 2014; Marleau *et al.* 2014). The appearance of this striking range of dynamical variation, both in the frequency and and quality of asynchrony among metacommunities shows the important role of the pattern of connections among local communities in shaping the regional dynamics of metacommunities.

Emergent asynchrony in nature

The emergence of complex asynchronous dynamics from homogeneous metacommunities makes it challenging to draw inferences about habitat quality based on community dynamics. As our results demonstrate, differences between communities may be driven by spatial patterns imposed by the structure of dispersal rather than any environmental effects, or a combination of both. Without accounting for the effects of spatial structure, approaches assuming that species distributions are driven primarily by environmental features may fail to accurately identify the importance of habitat patches for conservation or predict the effects of environmental changes on species (Keith *et al.* 2008; Swab *et al.* 2012). When spatial heterogeneity is produced through pattern formation, the structure as a whole is responsible for determining what patterns are possible and the resulting effects on species. Conservation planning that includes the addition or removal of habitat or connections between them must then consider the importance of these

mechanisms.

Additionally, we have demonstrated that while asynchrony generally provides enhanced stability for a community relative to synchrony, its effect varies depending on the spatial pattern of asynchrony. The relative strength of stabilizing effects vary both at the regional scale, as through spatial averaging and rescue effects, and at the local scale through dispersal subsidies depending on the patterns promoted by the spatial structure of the metacommunity. Plans to promote stability at the metacommunity level then must move beyond how to maintain asynchrony and consider the patterns of asynchrony and their overall effect on community dynamics.

Emergence of asynchronous dynamics

The emergence of the asynchronous equilibria we observe is an example of pattern formation, wherein stable heterogeneity emerges from a homogeneous system (Turing 1952). In these cases, variation in initial conditions provides a source of heterogeneity which is stabilized by the underlying structure of the environment and movement within it. While these are typically studied in the context of Turing instabilities, wherein spatial processes also destabilize the synchronized homogeneous state, alternative mechanisms for the formation of spatial patterns have been described (Cahn & Hilliard 1958; Liu *et al.* 2013), and they can occur in systems with locally stable homogeneous states (Wolfrum 2012). The patterns we observe are surprising because they are equivalent to the special case of traveling wave patterns as their equilibria are limit cycles rather than fixed points, which typically require at least three species to occur (Hata *et al.* 2014; Turing 1952). Here they can arise with only two species because the interaction between the predator and prey is already prone to oscillation (Yang *et al.* 2004). These dynamics are a prime example of emergent behavior, wherein the interactions between the components of a system give rise to collective dynamics which cannot be predicted by understanding the parts alone (Anderson *et al.* 1972). Despite each community patch in our simulations being identical when viewed individually, utilizing the same parameter values and connecting

to precisely four other patches, they can generate entirely different dynamics depending on the structure of the greater metacommunity and their position within it.

We describe the effects of this emergent asynchrony on the dynamics of metacommunities at both the local and regional scale. Total regional variability (Figure 2.3b) is determined both by the variability of individual patches and an additional reduction due to spatial averaging effects that result from phase differences among communities' limit cycles in our simulations (Goldwyn & Hastings 2008). Spatial averaging effects occur on the regional scale of the metacommunity, reducing total regional variability and extinction risk by buffering population minima with dispersal from populations at different points in their limit cycle (Briggs & M. F. Hoopes 2004; Maser *et al.* 2007). Spatial averaging does not cause changes at the local scale, however, and alone cannot be responsible for the differences in the dynamics among communities in the same metacommunity that we observe, as in Figure 2.3c. These differences are created by an additional interaction with the non-linearity of species' interactions, which causes the same relative amount of dispersal to have different effects on communities depending on their current position in their limit cycle. Dispersal can therefore simulate the effects of changing prey growth or predator attack rates and change the shape of communities' limit cycles (Briggs & M. F. Hoopes 2004; de Roos *et al.* 1998). The effect of dispersal on the shape of the limit cycle depends on the magnitude of dispersal between communities, which is increased by differences among communities. This feedback then causes the emergence of a heterogeneous spatial pattern if a stable pattern of differences among patches can be reached.

Spatial structure determines the emergence of stable asynchronous patterns from our homogeneous metacommunities primarily by constraining the spatial patterns possible. As discussed, in all observed spatial patterns all patches in a synchronized cluster are connected to the same type and number of other synchronized clusters. This arrangement is otherwise known as a balanced equivalence relation or balanced coloring, and is strictly required for the pattern of asynchrony to be stable (Theorem 6.5, Stewart *et al.* 2003). The number and corresponding pattern of these balanced colorings is specific to the

underlying spatial structure, dictating the number of synchronized clusters, a property which has been previously suggested to be the major determinant in differences between asynchronous metacommunities (Holland & Hastings 2008). However, we observe that metacommunities with different numbers of clusters can have identical stability properties and vice versa (Figure 2.3). Beyond influencing the synchronization of individual patches, structure also constrains how synchronized clusters of unique dynamics interact with one another. This indirectly determines the magnitude of dispersal experienced by each patch, a key driver of differences in the variability and limit cycles of each patch.

Conclusion

Overall, we find that characteristics of metacommunity spatial structure independent of connectivity play a crucial role in determining dynamics not only by influencing asynchrony frequency, but also by constraining the action of asynchrony's stabilizing mechanisms. Our findings suggest a need to both move beyond connectivity as the focus of spatial structure and to move beyond the presence or absence of synchrony to understand metacommunity dynamics. The spatial patterning of partially synchronized clusters is a major determinant of the effect of space on interactions between species. Considering that spatial structure is being dramatically altered as a result of human development and the importance of these mechanisms for maintaining stability of communities and persistence of species, a deeper understanding of the relationship between spatial structure, patterns of synchrony, and metacommunity dynamics is necessary both from a theoretical and conservation perspective.

Bibliography

Anderson, P. W. *et al.* (1972). More is different. *Science*, 177, 393–396.

Arenas, A., Dıaz-Guilera, A., Kurths, J., Moreno, Y. & Zhou, C. (2008). Synchronization in complex networks. *Physics Reports*, 469, 93–153.

Barahona, M. & Pecora, L. M. (2002). Synchronization in small-world systems. *Physical Review Letters*, 89, 054101.

Briggs, C. J. & Hoopes, M. F. (2004). Stabilizing effects in spatial parasitoid–host and predator–prey models: a review. *Theoretical population biology*, 65, 299–315.

Brown, J. H. & Kodric-Brown, A. (1977). Turnover rates in insular biogeography: effect of immigration on extinction. *Ecology*, 58, 445–449.

Buckling, A., Kassen, R., Bell, G. & Rainey, P. B. (2000). Disturbance and diversity in experimental microcosms. *Nature*, 408, 961–964.

Bunn, A. G., Urban, D. L. & Keitt, T. (2000). Landscape connectivity: a conservation application of graph theory. *Journal of Environmental Management*, 59, 265–278.

Cahn, J. W. & Hilliard, J. E. (1958). Free energy of a nonuniform system. I. Interfacial free energy. *The Journal of Chemical Physics*, 28, 258–267.

Chesson, P. & Huntly, N. (1997). The roles of harsh and fluctuating conditions in the dynamics of ecological communities. *The American Naturalist*, 150, 519–553.

Crooks, K. R. & Sanjayan, M. (2006). *Connectivity conservation*. Vol. 14. Cambridge University Press.

Csardi, G. & Nepusz, T. (2006). The igraph software package for complex network research. *InterJournal*, Complex Systems, 1695.

de Roos, A. M., McCauley, E. & Wilson, W. G. (1998). Pattern formation and the spatial scale of interaction between predators and their prey. *Theoretical population biology*, 53, 108–130.

Gilarranz, L. J. & Bascompte, J. (2012). Spatial network structure and metapopulation persistence. *Journal of Theoretical Biology*, 297, 11–16.

Goldwyn, E. E. & Hastings, A. (2008). When can dispersal synchronize populations? *Theoretical population biology*, 73, 395–402.

Gouhier, T. C., Guichard, F. & Gonzalez, A. (2010). Synchrony and stability of food webs in metacommunities. *The American Naturalist*, 175, E16–E34.

Hastings, A. (1993). Complex interactions between dispersal and dynamics: lessons from coupled logistic equations. *Ecology*, 1362–1372.

Hata, S., Nakao, H. & Mikhailov, A. S. (2014). Dispersal-induced destabilization of metapopulations and oscillatory Turing patterns in ecological networks. *Scientific Reports*, 4.

Holland, M. D. & Hastings, A. (2008). Strong effect of dispersal network structure on ecological dynamics. *Nature*, 456, 792–794.

Holyoak, M. & Lawler, S. P. (1996). Persistence of an extinction-prone predator-prey interaction through metapopulation dynamics. *Ecology*, 1867–1879.

Keith, D. A., Akçakaya, H. R., Thuiller, W., Midgley, G. F., Pearson, R. G., Phillips, S. J., *et al.* (2008). Predicting extinction risks under climate change: coupling stochastic population models with dynamic bioclimatic habitat models. *Biology Letters*, 4, 560–563.

Koelle, K. & Vandermeer, J. (2005). Dispersal-induced desynchronization: from metapopulations to metacommunities. *Ecology Letters*, 8, 167–175.

Leibold, M. A., Holyoak, M., Mouquet, N., Amarasekare, P., Chase, J., Hoopes, M., *et al.* (2004). The metacommunity concept: a framework for multi-scale community ecology. *Ecology Letters*, 7, 601–613.

Liebhold, A., Koenig, W. D. & Bjørnstad, O. N. (2004). Spatial synchrony in population dynamics. *Annual Review of Ecology, Evolution, and Systematics*, 467–490.

Liu, Q.-X., Doelman, A., Rottschäfer, V., Jager, M. de, Herman, P. M., Rietkerk, M. & Koppel, J. van de (2013). Phase separation explains a new class of self-organized spatial patterns in ecological systems. *Proceedings of the National Academy of Sciences*, 110, 11905–11910.

Marleau, J. N., Guichard, F. & Loreau, M. (2014). Meta-ecosystem dynamics and functioning on finite spatial networks. *Proceedings of the Royal Society of London B: Biological Sciences*, 281, 20132094.

Maser, G. L., Guichard, F. & McCann, K. S. (2007). Weak trophic interactions and the balance of enriched metacommunities. *Journal of Theoretical Biology*, 247, 337–345.

Murdoch, W. W., Briggs, C. J. & Nisbet, R. M. (2003). *Consumer-resource dynamics*. Vol. 36. Princeton University Press.

Paradis, E., Baillie, S., Sutherland, W. & Gregory, R. (1999). Dispersal and spatial scale affect synchrony in spatial population dynamics. *Ecology Letters*, 2, 114–120.

Plitzko, S. J. & Drossel, B. (2015). The effect of dispersal between patches on the stability of large trophic food webs. *Theoretical Ecology*, 8, 233–244.

Rosenzweig, M. L. & MacArthur, R. H. (1963). Graphical representation and stability conditions of predator-prey interactions. *The American Naturalist*, 209–223.

Saunders, D. A., Hobbs, R. J. & Margules, C. R. (1991). Biological consequences of ecosystem fragmentation: a review. *Conservation Biology*, 5, 18–32.

Soetaert, K., Petzoldt, T. & Setzer, R. W. (2010). Solving Differential Equations in R: Package deSolve. *Journal of Statistical Software*, 33, 1–25.

Steiner, C. F., Stockwell, R. D., Kalaimani, V. & Aqel, Z. (2011). Dispersal promotes compensatory dynamics and stability in forced metacommunities. *The American Naturalist*, 178, 159–170.

Stewart, I., Golubitsky, M. & Pivato, M. (2003). Symmetry groupoids and patterns of synchrony in coupled cell networks. *SIAM Journal on Applied Dynamical Systems*, 2, 609–646.

Swab, R. M., Regan, H. M., Keith, D. A., Regan, T. J. & Ooi, M. K. (2012). Niche models tell half the story: spatial context and life-history traits influence species responses to global change. *Journal of Biogeography*, 39, 1266–1277.

Taylor, P. D., Fahrig, L., Henein, K. & Merriam, G. (1993). Connectivity is a vital element of landscape structure. *Oikos*, 571–573.

Turing, A. M. (1952). The chemical basis of morphogenesis. *Philosophical Transactions of the Royal Society of London B: Biological Sciences*, 237, 37–72.

Watts, D. J. & Strogatz, S. H. (1998). Collective dynamics of 'small-world'networks. *Nature*, 393, 440–442.

Wolfrum, M. (2012). The Turing bifurcation in network systems: Collective patterns and single differentiated nodes. *Physica D: Nonlinear Phenomena*, 241, 1351–1357.

Yang, L., Zhabotinsky, A. M. & Epstein, I. R. (2004). Stable squares and other oscillatory Turing patterns in a reaction-diffusion model. *Physical Review Letters*, 92, 198303.

Chapter 3

Predicting pattern formation in multilayer networks

3.1 Introduction

The synchronization dynamics of systems of coupled oscillators play a central role in a tremendous range of phenomena across the physical, biological, and social sciences (Faloutsos *et al.* 1999; Freeman 1996; Holland & Hastings 2008; Jeong *et al.* 2000; Varela *et al.* 2001). A system of coupled oscillators can represent any dynamical system characterized by interactions between components with regular fluctuations in its state variables such as neurons, heart cells, animal populations, and power generators. Determining how and why oscillators in these systems either converge on the same set of dynamics (synchrony) or differentiate from one another (asynchrony) is central to our ability to both understanding and managing these types of systems (Albert & Barabási 2002; Boccaletti, Latora, *et al.* 2006; Strogatz 2001).

A valuable tool for investigating the synchronization dynamics of coupled oscillator systems has been the Kuramoto model, which features extremely simple and generalizable oscillator dynamics describing constant phase evolution following a sine wave and diffusion-based coupling between oscillators (Kuramoto 1975; Strogatz 2000).

However, due to the simplicity of the model the coupling of Kuramoto oscillators is only able to influence phase, while in many systems coupling also influences the internal dynamics of oscillators. Specifically, in multilayer networks where oscillations are produced by the interactions between multiple types of internal components, the coupling of like components between oscillators can cause differences in not only phase but also the amplitude of the oscillatory equilibrium. Thus the study of multilayer networks can reveal much about the role of structure in the synchronization dynamics in more complex real world systems (Boccaletti, Bianconi, *et al.* 2014).

Unsurprisingly, the synchronization dynamics of both single- and multi-layer oscillatory systems can be extremely complex. In the simplest case where every oscillator and their internal components are identical, total synchronization is expected and intuitive. However, even when oscillators are identical these systems are able to differentiate into a variety of dynamical regimes, reaching stable asynchronous equilibria: a phenomenon known as pattern formation (Cross & Hohenberg 1993; Turing 1952). These patterns are primarily known to be caused by Turing instabilities, wherein the synchronized, homogeneous state is destabilized by coupling between the components of the system (Turing 1952). It is not necessary for the synchronous state to be destabilized however; coupling among oscillators can also stabilize a variety of alternative asynchronous equilibria that coexist with the synchronous state (Nakao & Mikhailov 2010; Wolfrum 2012). In this case the equilibrium found by the system depends on initial conditions, and may shift with large enough perturbations depending on the landscape of equilibria and their attractive properties.

Despite the appearance of stable asynchronous equilibria even in the absence of Turing instability, pattern formation has been studied primarily by characterizing the stability of the synchronous state. Specifically, the Master Stability Function (MSF) formalism is commonly used to determine the conditions for stable synchrony in a given system and the general ability of individual structures to maintain synchrony (Arenas *et al.* 2008; Barahona & Pecora 2002; Pecora & Carroll 1998). This approach considers

the local stability of the synchronized equilibrium, particularly whether the system will return to synchrony following a small asynchronous perturbation. This tells us nothing about the number and qualities of asynchronous equilibria, however, as it considers a system's behavior only near the synchronous equilibrium. Studies on pattern formation in multilayer networks in particular have, so far, focused on the MSF and similar methods (Asllani *et al.* 2014; Hata *et al.* 2014; Kouvaris *et al.* 2015) for characterizing the stability of the synchronized state. Thus it is necessary to develop alternative approaches to further investigate the role of structure in the formation and stabilization of alternative asynchronous equilibria, particularly in multilayer networks.

Some approaches have been effective in illuminating the role of structure in the formation of asynchronous patterns, specifically in determining which patterns can emerge. For a pattern to be viable, the 'coloring' of oscillators (where oscillators with the same color are synchronized) must be balanced such that all oscillators of the same color are connected to the same numbers and colors of other oscillators (Stewart *et al.* 2003). A variety of methods for determining all the balanced colorings from a given structure have been developed (Aguiar & Dias 2014; Kamei & Cock 2013). From a balanced coloring a 'quotient network' can be constructed, illustrating the net interaction between colors of oscillators that results from a given pattern (Stewart *et al.* 2003). While these methods reveal much about how structure constrains asynchronous patterns, they are not able to predict how the dynamics of oscillators change due to asynchrony, which depends also on the dynamics of the individual oscillators and the nature of their interactions. Understanding and predicting the effect of structure on asynchronous multilayer network dynamics thus requires more detailed analysis.

To move beyond the focus on the stability of the synchronized state and investigate the effect of interaction structure on both the appearance and dynamics of alternative asynchronous equilibria, we develop and analyze a simple multilayer oscillator network model. We illustrate the use of this model in predicting the emergence and effect of asynchronous patterns on oscillator phase and amplitude by first analyzing the structure of

three oscillator networks. These systems are small enough to be solved effectively, while complex enough to provide insight into the mechanisms underlying pattern formation in more complex structures. Through this analysis we discuss how each oscillator's potential for differentiation is determined by its position within a network structure and the mechanisms underlying the differentiation of oscillator dynamics.

Finally, we compare the predictions of our model with the numerical results of a more complex multilayer model characterized by oscillations generated via nonlinear interactions among oscillator components. Our model successfully predicts many of the patterns generated by this more complex model, despite being significantly simpler. Overall our model provides a useful starting point for the analysis of pattern formation in multilayer networks which generalizes readily to more complex and realistic systems.

3.2 Multilayer Oscillator Network Model

Our multilayer oscillator network model is:

$$x_i' = \delta \sum_{j=1} L_{ij} r_j \cos(\theta_j - \theta_i) + \psi(1 - r_i) \tag{3.1}$$

$$y_i' = \delta \sum_{j=1} L_{ij} r_j \sin(\theta_j - \theta_i) \tag{3.2}$$

$$\theta_i' = \omega + \tan^{-1}(\frac{y_i'}{x_i'}) \tag{3.3}$$

$$r_i' = \sqrt{(r_i - x_i')^2 + y_i'^2} - r_i \tag{3.4}$$

We illustrate the components of our model in Figure 3.1. Our model is constructed similarly to the Kuramoto model (Kuramoto 1975), where θ_i is the phase of oscillator i and r_i its amplitude. Internally, each oscillator undergoes constant phase evolution ω around a limit cycle described by the unit circle, where the x dimension is $\cos(\theta)$ the y dimension is $\sin(\theta)$. Oscillators are coupled independently on both the x and y dimensions by the matrix L with coupling strength δ, such that δL_{ij} describes the effect of coupling from oscillator j on oscillator i. The matrix L is the negative Laplacian, or $A - D$

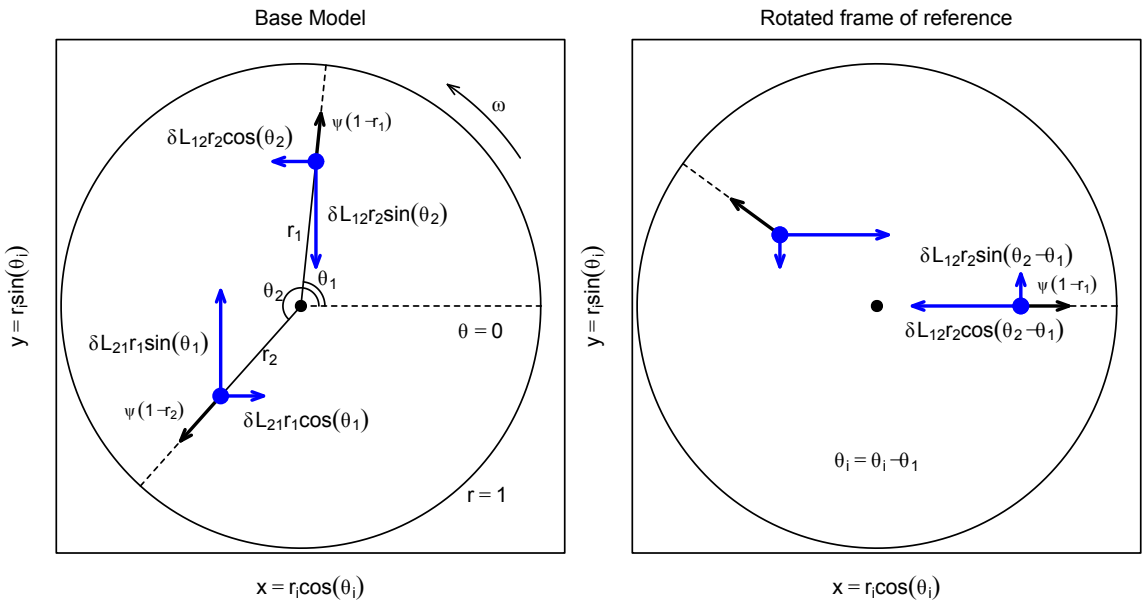

Figure 3.1: Illustration of the components of our multilayer oscillator network model. Each oscillator i is pulled toward the state of its neighbors j based on coupling strength δ and interaction strength L_{ji}, with the x and y dimensions acting as independent layers. Oscillators are also repelled from the center toward the intrinsic limit cycle based on the strength of repulsion ψ and distance from the intrinsic limit cycle $(1 - r_i)$. Calculations for the net effect of these forces on each oscillator i are simplified by rotating the frame of reference by oscillator i's phase such that the phase of all oscillators j, $\theta_j = \theta_j - \theta_i$, making $\theta_i = 0$, $y_i = 0$, and $x_i = r_i$.

where A is the adjacency matrix and D is the diagonal degree matrix. Thus, off-diagonal elements of L are positive while each diagonal element L_{ii} is the negative sum of the off-diagonal elements of row i.

Because oscillators are coupled on both the x and y dimensions amplitude r can vary, unlike the Kuramoto model. This allows oscillators to escape their intrinsic limit cycle ($r = 1$). To simulate the behavior of real limit cycles with unstable fixed points at their center, we introduce the parameter ψ for the repelling force of the center; the term $\psi(1 - r_i)$ causes amplitude r to move toward the limit cycle $r = 1$ at a fraction of ψ proportional to the oscillator's distance from the original limit cycle.

Calculations are simplified by rotating the frame of reference about the limit cycle by θ_i such that the phase of all oscillators j becomes $\theta_j = \theta_j - \theta_i$, making $\theta_i = 0$, $y_i = 0$, and $x_i = r$, as illustrated in Figure 3.1. It should be noted that this rotation

assumes that coupling strength δ and interaction structure L are the same for both the x and y dimensions of the oscillators. In our formulation of this model this holds true, however it is possible to alter the model such that interactions among oscillators differ between the x and y dimensions as they may for many multilayer systems. Additionally, the change in x and y dimensions shown in Eqns. 3.1 and 3.2 are changes post-rotation to simplify calculation of the change in phase and amplitude and thus do not represent the actual change in the x and y dimensions of each oscillator. Finally, as ω is constant (all oscillators are identical) we set $\omega = 0$ so that the only changes in phase analyzed are those relative to the phase of other oscillators and not intrinsic rotation about the limit cycle.

From Eqn. 3.3 we observe that the phase of oscillator i relative to the other oscillators is locked only if $y_i' = 0$, or:

$$\theta_i = \tan^{-1}\left(\frac{\sum_{j\neq i} L_{ij} r_j \sin(\theta_j)}{\sum_{j\neq i} L_{ij} r_j \cos(\theta_j)}\right) \tag{3.5}$$

This condition can be satisfied regardless of each oscillator's amplitude r_j or the strength of interactions L_{ij} if $\sin(\theta_j - \theta_i) = 0$ for all j, meaning $\theta_i = \theta_j \pm n\pi$, $n \in \mathbb{N}$ for all j. Alternatively, the sum of all interactions with other oscillators must balance to zero, or $\sum_{j\neq i} L_{ij} r_j \sin(\theta_j - \theta_i) = 0$.

From Eqn. 3.4, amplitude is locked when phase is locked ($y_i' = 0$) and $x_i = 0$, or:

$$r_i = \frac{\frac{\psi}{\delta} + \sum_{j\neq i} L_{ij} r_j \cos(\theta_j - \theta_i)}{\frac{\psi}{\delta} - L_{ii}} \tag{3.6}$$

With these conditions together, we can identify all equilibria present in a given system, including the trivial case of total synchrony ($\theta_i = 0$ and $r_i = 1$ for all i).

3.3 Three oscillator systems: equilibrium phases

To demonstrate the analysis of our model and shed light on the effects of structure on pattern formation, we analyze the effects of structure L on the equilibria of systems of three oscillators. There are two possible structures which connect all three oscil-

lators. The first is a triangle where every oscillator is connected to the other two, and the second is a line where two outer oscillators connect to a single middle oscillator. When describing phases, we rotate our point of reference about the unit circle such that the phase of each oscillator is described by their difference from the first oscillator, $\theta_i - \theta_1$. The first oscillator thus serves as our point of reference and is always 0 ($\theta_1 - \theta_1$). This simplifies analysis and highlights the differences between oscillator phases as the meaningful driver of dynamics.

As discussed, the condition for phase-locking (Eqn. 3.5) has a guaranteed solution independent of each oscillator's amplitude or the strength of interactions when $\sin(\theta_j - \theta_i) = 0$ for all i, j, or $\theta_i = \theta_j \pm n\pi,\ n \in \mathbb{N}$. As the period of each oscillator is 2π, π and $-\pi$ are equivalent and we have two possible phases for each oscillator: equal ($\theta_i - \theta_1 = 0$) or antiphase ($\theta_i - \theta_1 = \pm\pi$) to the first oscillator. This gives us three sets of asynchronous equilibrium phases for each structure, each with two oscillators sharing a phase and one antiphase to them. The amplitude of these oscillators can then be determined separately as we describe later.

Phases can also be locked when the effects of other oscillators on phase are balanced and cancel out; $L_{ij} r_j \sin(\theta_j - \theta_i) = -L_{ik} r_k \sin(\theta_k - \theta_i)$. Unlike the solutions with all phases equal or antiphase, these do depend on the strength of interactions and amplitude. This type of solution also requires that each oscillator have at least two connections to balance against each other, and as a result these equilibria are possible only for the triangle structure and not the line. We find by substitution the conditions for these equilibria:

$$L_{12}L_{23}L_{31} = L_{21}L_{32}L_{13} \tag{3.7}$$

$$\theta_2 - \theta_1 = \pm\cos^{-1}\left[\frac{(L_{23}L_{13}r_3)^2 - (L_{21}L_{13}r_1)^2 - (L_{12}L_{23}r_2)^2}{2(L_{21}L_{13}r_1)(L_{12}L_{23}r_2)}\right] \tag{3.8}$$

$$\theta_3 - \theta_1 = \mp\cos^{-1}\left[\frac{(L_{32}L_{12}r_2)^2 - (L_{31}L_{12}r_1)^2 - (L_{13}L_{32}r_3)^2}{2(L_{31}L_{12}r_1)(L_{13}L_{32}r_3)}\right] \tag{3.9}$$

The conditions specifying $\theta_2 - \theta_1$ and $\theta_3 - \theta_1$ turn out to be the equations for finding the angle of triangle from its sides, the law of cosines. In conjunction with a constraint on interaction structure, Eqn. 3.7, these conditions specify that phases are locked only

if the angles $\pi - (\theta_2 - \theta_1)$, $\pi - (\theta_3 - \theta_1)$, and $\pi - (\theta_3 - \theta_2)$ form a triangle with sides equal to the oscillator's amplitudes scaled by their interactions with other oscillators. The weighting of the sides of the triangle may differ between the equations for $\theta_2 - \theta_1$ and $\theta_3 - \theta_1$ as the first condition ensures that the angles of both triangles agree by requiring that all sides of the triangle for $\theta_3 - \theta_1$ are proportional to the sides of the triangle for $\theta_2 - \theta_1$ by $\frac{L_{23}}{L_{32}}$.

From these conditions we observe that phase-locking for these equilibria depends on ratios of amplitudes and interaction strengths, specifically $\frac{L_{ij}r_j}{L_{ik}r_k}$. Thus equilibrium phase can be determined independent of amplitude if the ratios remain constant, or $r_1' = r_2' = r_3'$. To illustrate, we consider the case of a triangle with equal interactions between all oscillators ($L_{ij} = 1$ for all i, j) and equal amplitudes for all oscillators, making $\frac{L_{ij}r_j}{L_{ik}r_k} = 1$ for all i, j, k. This satisfies the constraint on structure in Eqn. 3.7, and simplifies Eqns. 3.8 and 3.9 to $\theta_2 - \theta_1 = \pm\frac{2\pi}{3}$ and $\theta_3 - \theta_1 = \mp\frac{2\pi}{3}$. Following this, Eqn. 3.4 simplifies to $\frac{dr_i}{dt} = \delta(-3r_i) + \psi(1 - r_i)$, making the change in amplitude equal for all oscillators if the amplitudes are equal. Thus there is an asynchronous equilibrium at $r_1 = r_2 = r_3$ and $\theta_2 - \theta_1 = \pm\frac{2\pi}{3}$, and $\theta_3 - \theta_1 = \mp\frac{2\pi}{3}$.

From the conditions for phase-locking we find that structure plays a role in enabling the emergence of asynchronous equilibria on two levels. First, the 'qualitative' structure, or the presence/absence of interactions among oscillators, determines whether oscillators can be phase-locked without being equal or antiphase to each other. This effect immediately differentiates the line and triangle structures from one another, enabling a much wider range of possible asynchronous patterns for the triangle than for the line. Second, the 'quantitative' structure, or the strength of interactions among oscillators, provides an additional condition which must be met for equilibrium phases that are not equal or antiphase to be possible (Eqn. 3.7), and additionally plays a role in arbitrating the relationship between phase and amplitude in the more complex case of equilibria due to its appearance in the ratios $\frac{L_{ij}r_j}{L_{ik}r_k}$ (Eqns. 3.8, 3.9).

Overall, oscillators with more neighbors to interact with have more possibilities

Table 3.1: Calculated amplitudes for selected asynchronous equilibria. The parameters used were equal interaction strengths for all interactions ($L_{ij} = 1$ for all i, j), $\delta = .1$, and $\psi = .7$. For the line structure, oscillators 1 and 3 are at the ends and do not connect to each other ($L_{13} = L_{31} = 0$) while oscillator 2 is the middle connected to both. For the triangle structure each oscillator is equivalent due to equal weighting of interactions.

$\theta_2 - \theta_1$	$\theta_3 - \theta_1$	r_1 (end)	r_2 (mid.)	r_3 (end)
Line Structure				
0	$\pm\pi$	.975	.8	.775
$\pm\pi$	0	.8	.6	.8
$\pm\pi$	$\pm\pi$	.775	.8	.975
Triangle Structure				
0	$\pm\pi$	.8	.8	.6
$\pm\pi$	0	.8	.6	.8
$\pm\pi$	$\pm\pi$	.6	.8	.8
$\pm 2\pi/3$	$\mp 2\pi/3$	.7	.7	.7

for differentiation. An oscillator with a single interaction must be equal in phase or antiphase with its neighbor, while an oscillator with two neighbors can also be phase-locked if the neighbor's effects cancel out. The complexity of possible pattern formation mechanisms continues to scale with the number of oscillators and interactions; an oscillator with three neighbors can be phase-locked by having one neighbor cancel the other two, by being antiphase or equal to one and having the other two cancel, and so on. As a result, the number of possible asynchronous patterns can be expected to scale with the complexity of the network.

3.4 Three oscillator systems: equilibrium amplitudes

Next we consider how interaction structure L influences the amplitude of oscillators, first by analyzing the conditions for amplitude locking, found through substitution of Equation 3.6:

$$r_i = \frac{\psi^3 + \psi^2\delta F(i) + \psi\delta^2 G(i)}{\psi^3 + \psi^2\delta H_1 + \psi\delta^2 H_2 + \delta^3 H_3} \tag{3.10}$$

$$B_{ij} = L_{ij}\cos(\theta_i - \theta_j)$$

$$F(i) = (B_{ij} + B_{ik}) - (B_{jj} + B_{kk}) \qquad H_1 = -(B_{11} + B_{22} + B_{33})$$

$$G(i) = (B_{kj}B_{ik} + B_{ij}B_{jk} + B_{jj}B_{kk}) \qquad H_2 = (B_{11}B_{22} + B_{11}B_{33} + B_{22}B_{33})$$

$$- (B_{ij}B_{kk} + B_{jj}B_{ik} + B_{jk}B_{kj}) \qquad - (B_{12}B_{21} + B_{13}B_{31} + B_{23}B_{32})$$

$$H_3 = (B_{33}B_{12}B_{21} + B_{22}B_{13}B_{31} + B_{11}B_{23}B_{32})$$

$$- (B_{11}B_{22}B_{33} + B_{12}B_{23}B_{31} + B_{21}B_{13}B_{32})$$

The terms of Equation 3.10 are made up of combinations of elements B, a matrix combining the effect of phase differences and the matrix of interaction strengths between oscillators L. Of these terms, $F(i)$ and $G(i)$ can differ for each oscillator while H_1, H_2, and H_3 will be constant for all oscillators in the system.

In the cases where phase is locked independently from amplitude, amplitude is straightforward to calculate using the parameters of the system. To illustrate we show examples of the calculated amplitude for each of the equilibrium phases we identified in the previous section in Table 3.1, where interactions are equal among all oscillators for both structures ($L_{ij} = 1$ for all i, j). These results highlight an interesting difference between the line and triangle structures: for the triangle, oscillators with equal phases have the same amplitude, while oscillators at the end of the line structure (1 & 3) have differing amplitudes when phase is equal to the middle oscillator. Thus, despite oscillators in the line structure being constrained to two phases all three are able to differentiate and avoid total synchronization with their neighbors.

We can determine the conditions for oscillators with equal phase to exhibit different amplitudes by determining whether $F(i) = F(j)$ and $G(i) = G(j)$ in Equation 3.10. In particular, for two oscillators to maintain different amplitudes while sharing the same

phase, at least one of these conditions must be false:

$$\begin{aligned} F(i) = F(j) \leftrightarrow & (B_{ij} + B_{ik}) - (B_{ji} + B_{jk}) = 0 \\ G(i) = G(j) \leftrightarrow & B_{ik}[(B_{ki} + B_{kj}) - (B_{ji} + B_{jj})] + \\ & B_{jk}[(B_{ii} + B_{ij}) - (B_{ki} + B_{kj})] + \\ & B_{kk}[(B_{ji} + B_{jj}) - (B_{ii} + B_{ij})] = 0 \end{aligned}$$

These conditions will always be true if the set of interactions both to and from the two oscillators i and j are isomorphic, or $B_{i.} \cong B_{j.} \rightarrow F(i) = F(j)$, $B_{.i} \cong B_{.j} \rightarrow G(i) = G(j)$. As we observed, when interactions are equal among all oscillators ($L_{ij} = 1$ for all i, j), all oscillators are isomorphic in the triangle structure, and thus will have the same amplitude if phase is equal. For the line structure, the two ends are isomorphic while the center is not, and so as we observed the ends will share the same amplitude if their phase is equal while the amplitude of the ends will differ from the middle when phase is equal.

From this the symmetry of an interactions structure, which is defined by the automorphisms of the interaction structure, is shown to play a significant role in constraining the types of asynchronous patterns possible. The ability to maintain differences in dynamics among oscillators with the same phase through variation in amplitude can create a variety of patterns unique to multilayer networks, however this is not possible between oscillators which are isomorphic. As a result, the addition or removal of links which increase the symmetry of an interaction structure prevents the formation of certain patterns, as observed in our comparison between the line and triangle structures. Overall, structures with low self-symmetry but a high degree of connectance among oscillators are expected to foster the greatest number of possible asynchronous patterns.

By further analyzing Equation 3.10 we can identify the specific elements of structure that drive of differences in amplitude between oscillators. First, we observe that the terms of this equation correspond to important subcomponents of the matrix B, where $B_{ij} = L_{ij}\cos(\theta_i - \theta_j)$, specifically the determinant $\det(B)$ trace, $\mathrm{tr}(B) = \sum B_{ii}$ and cofactors

$C_{ij} = (-1)^{i+j}\det(D_{ij})$, where D_{ij} is a submatrix of B with row i and column j removed:

$$F(i) = \sum_{j=1}(B_{ij}) - \mathrm{tr}(B) \qquad H_1 = -\mathrm{tr}(B)$$

$$G(i) = \sum_{j=1} C_{ji} \qquad H_2 = \sum_{j=1} C_{jj}$$

$$H_3 = -\det(B)$$

As $L_{ii} = -\sum_{j\neq i} L_{ji}$, the sum of all columns of L equals 0. Therefore when all phases are equal $L = B$, making $F(i) = H_1$, $G(i) = H_2$, and $H_3 = 0$, thus $r = 1$ for all oscillators. This corresponds to our case of total synchrony with no deviation in amplitude from the original limit cycle.

The conditions which maximize change in amplitude from the basal state $r = 1$ can be found by minimizing $F(i)$ and $G(i)$ and maximizing H_1, H_2, and H_3. $F(i)$ and H_1 both depend on the negative sum of the diagonal elements of the coupling matrix L, which is the total of all interaction strengths in the system. High total interaction strengths increase both H_1 and $F(i)$, however $F(i)$ is not affected by the value of L_{ii}. $F(i)$ can also be reduced independently from H_1 by phase differences greater than $\pi/2$ and less than $3\pi/2$ between oscillator i and its neighbors, which make the elements B_{ij} negative. $F(i)$ is minimized for a given interaction matrix when oscillator i is antiphase with its neighbors, as in the two cluster solutions of Table 3.1. $F(i)$ is then further reduced the greater the strength of interaction with antiphase neighbors.

Next, $G(i)$ and H_2 depend on the cofactors of B. For H_2, the cofactors are the determinants of the matrices describing the coupling between each pair of oscillators. For cofactor i, i this value is

$$C_{ii} = (L_{jj}L_{kk}) - (L_{jk}L_{kj})\cos^2(\theta_j - \theta_k) \tag{3.11}$$

The maximum for each of these values is $L_{jj}L_{kk}$, which is realized either when L_{jk} and/or $L_{kj}$is zero or when $\theta_j - \theta_k = \pi/2 \pm n\pi,\ n \in \mathbb{N}$. In cases where all oscillators are equal or antiphase, this simplifies to $(L_{jj}L_{kk}) - (L_{jk}L_{kj})$ as $\cos^2(\pi) = \cos^2(0) = 1$. Substituting

$L_{ii} = -\sum_{j \neq i} L_{ij}$, cofactor i, i becomes $L_{ji}L_{ki} + L_{ji}L_{kj} + L_{jk}L_{ki}$, illustrating the dependence of these values on interactions with the third oscillator, i. In cases where the phases of oscillators are locked by balancing their interactions, each cofactor is increased the closer $\theta_j - \theta_k$ is to $\pi/2 \pm n\pi,\ n \in \mathbb{N}$, which also corresponds to an increasing effect of oscillators j and k on the other's phase, requiring an equally strong opposing effect for phase to be locked. Overall H_2 is increased by balanced interactions among oscillators.

The cofactors determining $G(i)$ include one of the cofactors from H_2, C_{ii}, the determinant of the coupling matrix between j and k. $G(i)$ also includes the signed determinants of the other submatrices constructed from L with column i removed. Cofactor j, i is

$$C_{ji} = L_{ij}L_{jk}\cos(\theta_i - \theta_j)\cos(\theta_j - \theta_k) - L_{jj}L_{ik}\cos(\theta_i - \theta_k) \tag{3.12}$$

The minimum for these cofactors is $-(L_{ji}L_{ik} + L_{jk}L_{ik} + L_{ij}L_{jk})$, as $L_{jj} = -\sum_{i \neq j} L_{ij}$. This occurs for a given interaction matrix when i is antiphase with both j and k, or $\theta_i - \theta_j$ and $\theta_i - \theta_k$ equals $\pi \pm n2\pi,\ n \in \mathbb{N}$, and $\theta_j - \theta_k$ equals zero. Both C_{ji} and C_{ki} are minimized by these phase differences. These conditions are similar to those that minimize $F(i)$, however $G(i)$ is also minimized by strong interactions between its two neighbors, L_{jk} and L_{kj}, and high total interaction strength for each, L_{jj} and L_{kk}.

Finally, H_3 is the negative determinant of B. This value expands to

$$\begin{aligned}
-\det(B) = {} & L_{ij}L_{ji}(L_{ki} + L_{kj})(1 - \cos^2(\theta_i - \theta_j)) && (3.13)\\
& + L_{ik}L_{ki}(L_{ji} + L_{jk})(1 - \cos^2(\theta_i - \theta_k)) && (3.14)\\
& + L_{jk}L_{kj}(L_{ij} + L_{ik})(1 - \cos^2(\theta_j - \theta_k)) && (3.15)\\
& + (L_{ij}L_{jk}L_{ki} + L_{ik}L_{kj}L_{ji})(1 - \cos(\theta_i - \theta_j)\cos(\theta_i - \theta_k)\cos(\theta_j - \theta_k)) && (3.16)
\end{aligned}$$

Maximizing H_3 depends on the specific interaction matrix, as no one set of phase differences can maximize $1 - \cos^2(\theta_i - \theta_j)$ for all i, j. In the case where all interaction strengths are equal, $L_{ij} = 1$ for all i, j, H_3 is maximized when $\theta_j - \theta_i = \pm 2\pi/3$ and $\theta_k - \theta_i = \mp 2\pi/3$, the triangle's three cluster equilibrium in Table 3.1. In this case, H_3

like H_2 is increased by even phase differences among oscillators due to the evenly distributed interaction strengths between oscillators. In other cases, the maximum for H_3 will shift such that oscillators with stronger interactions ($L_{ij}L_{ji}$) should have phase differences closer to $\pi/2 \pm n\pi,\ n \in \mathbb{N}$, making $\cos^2(\theta_i - \theta_j)$ closer to zero and indicating a stronger effect of i and j on eachother's phase.

Altogether, these conditions provide insight into the mechanisms by which interaction structure changes oscillator dynamics. System-wide reductions in amplitude are promoted by high total interaction strengths (H_1), evenly distributed interactions among oscillators (H_2), and phase differences which match the pattern of interactions among oscillators (H_3). Curiously, both high total interaction strength and even distribution of interaction strengths are both known to promote synchrony (Arenas *et al.* 2008; Watts & Strogatz 1998). This may not be surprising, as the conditions which maximize differences in amplitude also suggest strong effects of oscillators on one another which promotes synchronization. This presents an interesting trade-off in maximizing either the frequency of asynchrony, in terms of the range of initial conditions which will lead to asynchrony, versus the strength of the effect of asynchrony on oscillator amplitude.

In addition to the aforementioned system-wide effects, $F(i)$ and $G(i)$ describe the conditions which influence the amplitudes of individual oscillators. Specifically, oscillator i's amplitude is reduced by strong interactions with neighbors j and k when both have high phase differences with i. Additionally, strong interactions and low phase differences between j and k reduce i's amplitude. These effects compete with the system-wide effects on amplitude: the conditions which minimize $F(i)$ and $G(i)$ have all oscillators are equal or antiphase, constraining H_3 to zero and limiting H_2. The ultimate effect of each of these terms on amplitude depends on the center resistance ψ and coupling strength δ. Higher values of coupling strength δ increase the effect of H_3 in particular and the effect of $G(i)$ and H_2 relative to $F(i)$ and H_1 respectively. Higher values of center resistance ψ have the opposite effect, having no effect on H_3 while increasing $F(i)$ and H_1 relative to $G(i)$ and

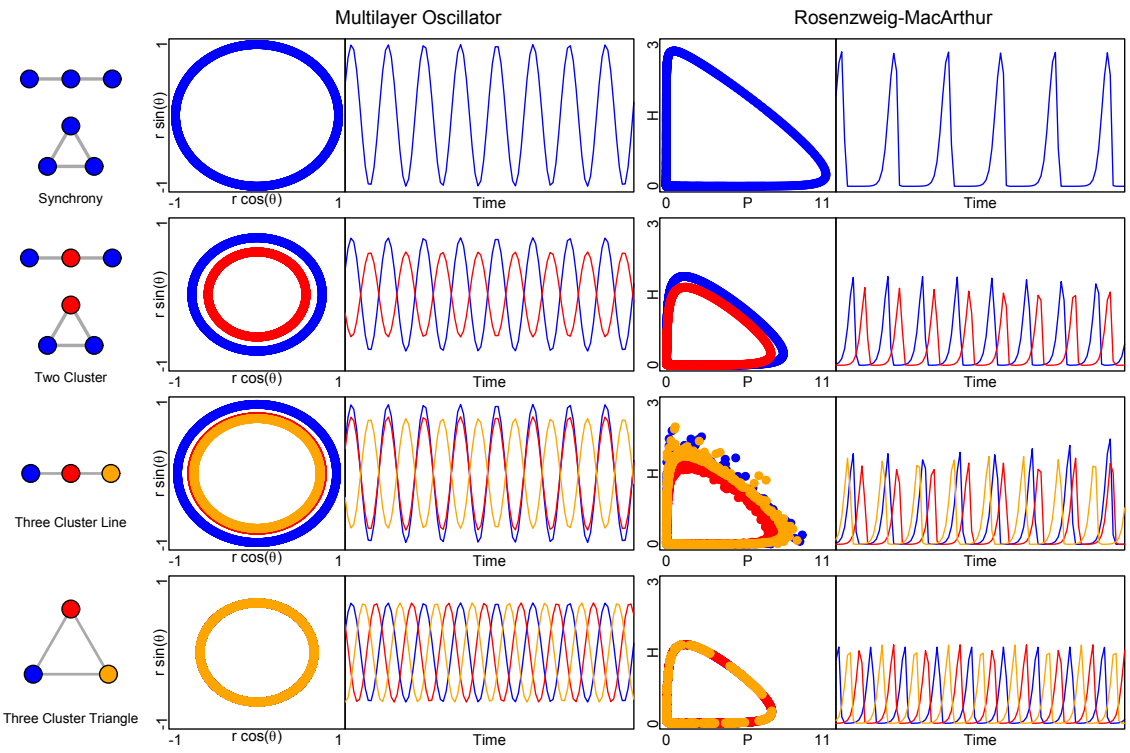

Figure 3.2: Comparison between the asynchronous states observed in the Rosenzweig-MacArthur model and our multilayer oscillator model. Simulations were run until dynamics were stationary for 5000 timesteps. We used the parameters $\omega = .5$, $\delta = .1$, and $\psi = .7$ for the multilayer model and $K = .3$, $e = 5$, $m = 1$, and $\delta = .001$ for the Rosenzweig-MacArthur model. The two three-oscillator interaction structures were used, a line and a triangle, both with $L_{ij} = 1$ for all i, j. Initial conditions known to produce asynchrony in the multilayer model were used, with $r = 1$ and $\theta = [0, 0, 0]$ for synchrony, $[0, \pi, 0]$ for two clusters, $[0, 0, \pi]$ for three clusters on the line, and $[0, 2\pi/3, -2\pi/3]$ for three clusters on the triangle. For the Rosenzweig-MacArthur model, the same initial conditions were translated into the x and y dimensions, with amplitude rescaled and centered around the limit cycle, predator abundance $p_i = \hat{p} + r_i \cos(\theta_i) +$ and prey $h_i = \hat{h} + .25 r_i \sin(\theta_i)$.

H_2.

Simulation results and comparison with ecological model

We compare the dynamics of our model with a commonly studied and more complex ecological model, the Rosenzweig-MacArthur predator-prey model (Rosenzweig & MacArthur 1963). Specifically, we use a non-dimensional form with dispersal between sub-populations of predators and prey, which has previously been used to study the

effects of structure on dynamics (Holland & Hastings 2008):

$$h_i' = h_i(1 - h_i K) - \frac{p_i h_i}{1 + h_i} + \delta \sum_{j=1}^{n} L_{ij} h_j \tag{3.17}$$

$$p_i' = \frac{e p_i h_i}{1 + h_i} - m p_i + \delta \sum_{j=1}^{n} L_{ij} p_j \tag{3.18}$$

Where h_i and p_i are the abundance of prey and predators respectively in sub-population i, K represents prey self-regulation, e the intensity of predation, and m predator mortality. L is the structure of movement among subpopulations and δ the rate of movement, both of which are equivalent to the structure L and strength δ of coupling among oscillators in our model. In comparing the two models, each subpopulation of predator and prey are equivalent to the x and y dimensions of an oscillator. The limit cycle of the predators and prey is centered around the system's unstable fixed point, $\hat{h} = m(e - m)$ and $\hat{p} = (1 + \hat{h})(1 - \hat{h}K)$.

Between the two models, interactions between oscillators are the same while each differs in terms of the local dynamics generating oscillations. While the simple limit cycle followed by our general multilayer model is contrived by the construction of the, the Rosenzweig-MacArthur model's limit cycle is an emergent property of non-linear interaction between the predator and prey, specifically $(p_i h_i)/(1 + h_i)$. Thus our comparison is intended to illustrate the degree to which interactions in oscillators alone can be used to predict the emergence of asynchronous states which generalize across different types of local dynamics.

We compare the asynchronous states exhibited and dynamics produced by both models in Figure 3.2. Despite the different shape of limit cycle and intrinsic nonlinearity of the ecological model, the asynchronous states it produces and their dynamics resemble those found in our multilayer oscillator model. In particular, the pattern of phases and amplitudes of the two cluster and three cluster triangle equilibria are very similar, demonstrating similar mechanisms underlying the formation of asynchronous equilibria in both models. Specifically, we observe the action of both the phase-locking of antiphase oscillators (Fig. 3.2 Two Cluster) and the balancing of phase differences to produce

Table 3.2: Cycle periods for each oscillator in all equilibria observed in the Rosenzweig-MacArthur model. Periods were calculated from the last 500 timesteps of each simulation as the difference in timing between cycle maxima. The estimate of the time of each maximum was improved using quadratic interpolation.

Equilibrium Type	Oscillator	Min. Period	Mean Period	Max. Period
Synchrony	Blue	18.33	18.49	18.66
Two Cluster	Blue	12.04	12.09	12.19
	Red	12.05	12.08	12.20
Three Cluster Line	Blue	12.06	12.27	13.91
	Red	11.29	12.17	12.71
	Orange	12.05	12.43	15.68
Three Cluster Triangle	Blue	11.31	11.50	11.68
	Red	11.42	11.50	11.57
	Orange	11.30	11.50	11.69

asynchronous equilibria (Fig. 3.2 Three Cluster Triangle) in the Rosenzweig-MacArthur predator-prey model.

By contrast we note substantial differences in the equilibria produced by the multilayer oscillator and Rosenzweig-MacArthur for the three cluster line treatment. While the Rosenzweig-MacArthur model is asynchronous in this case, the amplitudes of each oscillator do not follow the expected pattern and differences in phase are irregular. Irregularity in phase difference occurs due to differences in the period of each oscillator's limit cycle, a feature of the Rosenzweig-MacArthur model not accounted for in our model. In the multilayer oscillator model, the phase evolution of each oscillator is fixed and equal (ω), locking each oscillator to the same period of fluctuations regardless of any other details about the state of the system. In the Rosenzweig-MacArthur model, oscillations depend on the non-linear interaction between prey h_i and predators p_i, leading to a great deal of potential variation in period. We illustrate this variation in Table 3.2 by summarizing the periods of oscillations observed in each equilibria for the Rosenzweig-MacArthur model. In particular we note that the period of each oscillator is the same for the two cluster and three cluster triangle equilibria, which agree with the predictions of the multilayer oscillator model, while the period of each oscillator varies dramatically for the three cluster line equilibrium.

While our model offers a simplified look at the effect of interaction structure between oscillators on the formation of asynchronous equilibria, many of its features can be readily generalized to more complex systems. Without modification it successfully predicts the pattern of amplitudes and phases of several of the more complex model's equilibria. While it fails to predict the pattern of amplitudes and phases of the three cluster line equilibrium, it is still effective at predicting the conditions which lead to asynchronous equilibria in all three tested cases. Further adjustments to the model, specifically changing the rate of phase evolution ω to depend on the cycle's amplitude or phase, could be used capture the effect of non-linearities on cycle period. Overall, the generalizability of many of our results recommends our approach as a useful starting point for the analysis of the effects of interaction structure on the appearance of asynchronous equilibria in these systems.

3.5 Conclusions

Through the analysis of our relatively simple multilayer oscillator model we have illustrated the conditions underlying pattern formation on multilayer networks and provided methods for predicting the asynchronous dynamics of coupled oscillators based on their interaction structure. In particular we highlight several mechanisms governing the appearance of asynchronous equilibria in these networks. In the first case, the phases of oscillators which are antiphase ($\theta_i - \theta_j = \pi$) do not influence each other and will cause the amplitude of both patches to decrease (Figure 3.2: Two Cluster). In the second, oscillators with the same phase may differ in terms of amplitude if the positions of the two oscillators in the interaction structure are not isomorphic (Figure 3.2: Three Cluster Line). Finally, an oscillator's phase may be locked if the effects of the oscillators with which it interacts are equal and opposite, or otherwise balance to zero (Figure 3.2: Three Cluster Triangle). This mechanism has the potential to produce the most variable type and number of asynchronous dynamics while also being the most challenging to predict,

as, unlike the previous mechanisms, phase-locking depends also on the amplitudes of each oscillator relative to their neighbors.

Our analysis of three oscillator systems also reveals several properties of the structure of interactions among oscillators which determine the amplitude of oscillators for asynchronous equilibria. These properties act on two scales, affecting oscillators individually and affecting the entire system uniformly. For an individual oscillator, amplitude is influenced most by strong interactions with neighbors with large differences in phase. Individual oscillators are also affected indirectly by interactions of other oscillators with its neighbors. In these cases amplitude is affected most strongly when phase differences or interactions between a neighbor and its neighbors are small or weak. Finally, the amplitudes of all oscillators in a system are affected equally by the total dispersal of each oscillator, the cofactors describing coupling between each pair of oscillators, and the determinant of the matrix combining the effects of interaction strength and phase difference $B = L_{ij}\cos(\theta_i - \theta_j)$. The effects on amplitude at each scale compete with one another: individual differences in amplitude among oscillators are highest when there is no system-wide effect and vice-versa. These effects are also influenced by the overall strength of coupling δ and the repelling force of the limit cycle's center ψ. All effects increase with coupling strength δ, however indirect effects and the system-wide effect on amplitude are influenced more strongly. Conversely, direct effects scale exponentially with the center's repelling force ψ while indirect effects scale linearly and system-wide effects are not influenced. Altogether our analysis of these effects of interaction structure on oscillator amplitude provides valuable insight into the drivers of differentiation among multilayer oscillator systems during pattern formation.

Overall, the analysis of our model presents a wider view of the mechanisms underlying the formation of asynchronous patterns by investigating the effects of structure on asynchronous equilibria. Our methods can be applied to inform the design of interacting systems to minimize asynchronous pattern formation where this is desired, such as in power grids (Sachtjen *et al.* 2000) and wireless communication (Díaz-Guilera & Arenas

2008). Alternatively, our methods describe how the differentiating effects of asynchronous patterns can be predicted and manipulated through the structure of interactions for other applications, such as studies of brain function (Uhlhaas *et al.* 2010) and reserve design in ecology (Holyoak & Fahrig 2000).

Bibliography

Aguiar, M. A. & Dias, A. P. S. (2014). The lattice of synchrony subspaces of a coupled cell network: Characterization and computation algorithm. *Journal of Nonlinear Science*, 24, 949–996.

Albert, R. & Barabási, A.-L. (2002). Statistical mechanics of complex networks. *Reviews of Modern Physics*, 74, 47.

Arenas, A., Dıaz-Guilera, A., Kurths, J., Moreno, Y. & Zhou, C. (2008). Synchronization in complex networks. *Physics Reports*, 469, 93–153.

Asllani, M., Busiello, D. M., Carletti, T., Fanelli, D. & Planchon, G. (2014). Turing patterns in multiplex networks. *Physical Review E*, 90, 042814.

Barahona, M. & Pecora, L. M. (2002). Synchronization in small-world systems. *Physical Review Letters*, 89, 054101.

Boccaletti, S., Bianconi, G., Criado, R., Del Genio, C. I., Gómez-Gardenes, J., Romance, M., *et al.* (2014). The structure and dynamics of multilayer networks. *Physics Reports*, 544, 1–122.

Boccaletti, S., Latora, V., Moreno, Y., Chavez, M. & Hwang, D.-U. (2006). Complex networks: Structure and dynamics. *Physics Reports*, 424, 175–308.

Cross, M. C. & Hohenberg, P. C. (1993). Pattern formation outside of equilibrium. *Reviews of Modern Physics*, 65, 851.

Díaz-Guilera, A. & Arenas, A. (2008). Phase patterns of coupled oscillators with application to wireless communication. In: *Bio-Inspired Computing and Communication* (ed.). Springer, pp. 184–191.

Faloutsos, M., Faloutsos, P. & Faloutsos, C. (1999). On power-law relationships of the internet topology. In: *ACM SIGCOMM computer communication review*. Vol. 29. 4. ACM, pp. 251–262.

Freeman, L. C. (1996). Some antecedents of social network analysis. *Connections*, 19, 39–42.

Hata, S., Nakao, H. & Mikhailov, A. S. (2014). Dispersal-induced destabilization of metapopulations and oscillatory Turing patterns in ecological networks. *Scientific Reports*, 4.

Holland, M. D. & Hastings, A. (2008). Strong effect of dispersal network structure on ecological dynamics. *Nature*, 456, 792–794.

Holyoak, M. & Fahrig, L. (2000). Habitat patch arrangement and metapopulation persistence of predators and prey. *The American Naturalist*, 156, 378–389.

Jeong, H., Tombor, B., Albert, R., Oltvai, Z. N. & Barabási, A.-L. (2000). The large-scale organization of metabolic networks. *Nature*, 407, 651–654.

Kamei, H. & Cock, P. J. (2013). Computation of balanced equivalence relations and their lattice for a coupled cell network. *SIAM Journal on Applied Dynamical Systems*, 12, 352–382.

Kouvaris, N. E., Hata, S. & Díaz-Guilera, A. (2015). Pattern formation in multiplex networks. *Scientific Reports*, 5.

Kuramoto, Y. (1975). Self-entrainment of a population of coupled non-linear oscillators. In: *International symposium on mathematical problems in theoretical physics*. Springer, pp. 420–422.

Nakao, H. & Mikhailov, A. S. (2010). Turing patterns in network-organized activator-inhibitor systems. *Nature Physics*, 6, 544–550.

Pecora, L. M. & Carroll, T. L. (1998). Master stability functions for synchronized coupled systems. *Physical Review Letters*, 80, 2109.

Rosenzweig, M. L. & MacArthur, R. H. (1963). Graphical representation and stability conditions of predator-prey interactions. *The American Naturalist*, 209–223.

Sachtjen, M., Carreras, B. & Lynch, V. (2000). Disturbances in a power transmission system. *Physical Review E*, 61, 4877.

Stewart, I., Golubitsky, M. & Pivato, M. (2003). Symmetry groupoids and patterns of synchrony in coupled cell networks. *SIAM Journal on Applied Dynamical Systems*, 2, 609–646.

Strogatz, S. H. (2000). From Kuramoto to Crawford: exploring the onset of synchronization in populations of coupled oscillators. *Physica D: Nonlinear Phenomena*, 143, 1–20.

Strogatz, S. H. (2001). Exploring complex networks. *Nature*, 410, 268–276.

Turing, A. M. (1952). The chemical basis of morphogenesis. *Philosophical Transactions of the Royal Society of London B: Biological Sciences*, 237, 37–72.

Uhlhaas, P. J., Roux, F., Rodriguez, E., Rotarska-Jagiela, A. & Singer, W. (2010). Neural synchrony and the development of cortical networks. *Trends in Cognitive Sciences*, 14, 72–80.

Varela, F., Lachaux, J.-P., Rodriguez, E. & Martinerie, J. (2001). The brainweb: phase synchronization and large-scale integration. *Nature Reviews Neuroscience*, 2, 229–239.

Watts, D. J. & Strogatz, S. H. (1998). Collective dynamics of 'small-world'networks. *Nature*, 393, 440–442.

Wolfrum, M. (2012). The Turing bifurcation in network systems: Collective patterns and single differentiated nodes. *Physica D: Nonlinear Phenomena*, 241, 1351–1357.

Chapter 4

Persistence of isolated food webs does not predict persistence of spatial food webs

4.1 Introduction

Identifying the mechanisms that allow large, complex food webs to persist has been a central goal of ecology since the work of Robert May (1972) first identified the challenges that complexity imposes on the coexistence of species in trophic communities. Many properties of food web structure have been shown to play a major role in species persistence, including high ratios of consumer to resource body mass (Brose *et al.* 2006; Kartascheff *et al.* 2010). However, while these persistence mechanisms have historically studied in the context of individual, isolated food webs, more recently it has been well demonstrated that food webs can take advantage of alternative persistence mechanisms when connected in space with other food webs by the dispersal of organisms (Briggs & M. F. Hoopes 2004; Leibold *et al.* 2004). While these spatial persistence mechanisms have received a great deal of study in recent years, it is not clear how they interact with isolated persistence mechanisms such as those related to food web structure. Here we

investigate specifically how differences in the structure of food web influence their ability to benefit from spatial persistence mechanisms and how this relates to ability to persist when isolated.

The spatial persistence mechanisms enabled by dispersal from neighboring food webs range from the rescue of extinction-prone species (Brown & Kodric-Brown 1977), to reducing population variability through averaging effects (Maser *et al.* 2007), to reducing the effect of disturbances (Buckling *et al.* 2000; Chesson & Huntly 1997). For dispersal to have any effect however, it is also necessary that the trophic communities within the metacommunity differ. For populations to be rescued by neighbors from extinction, the times at which neighboring populations are vulnerable must be staggered, requiring differences in the timing of fluctuations in abundance among neighbors. Dispersal from populations with lower variability and extinction risk can also moderate the fluctuations of highly variable or extinction prone neighbors. These differences in timing and dynamics, or 'asynchrony', are thus a critical component of the spatial persistence mechanisms relied upon by many complex food webs in nature (Gouhier *et al.* 2010; Steiner *et al.* 2011). Thus to understand the relationship between food web structure and spatial persistence mechanisms we are primarily concerned with understanding how food web structure influences their tendency to be synchronous or asynchronous when spatial.

Thus far spatial persistence mechanisms and asynchrony have primarily been studied for small food web modules (Amarasekare 2008; Marleau *et al.* 2014) due to the many inherent challenges both in formulating realistic models with large numbers of interacting species and in characterizing the dynamics of large food webs. Studies that have considered more complex food webs suggest strongly that spatial interactions influence species in ways that may not be readily predictable from analysis of food webs in isolation and may confound traditional expectations, particularly by inverting the expected negative complexity-stability relationship (Mougi & Kondoh 2016; Plitzko & Drossel 2015). These studies have tended to aggregate food webs by the number of species or patches in their analyses however, leaving it unclear how the action of spatial persistence mecha-

nisms and tendency to be asynchronous differs between food web structures.

Thus, to further investigate the effect of food web structure on asynchrony frequency we utilize an allometric modeling framework (Brose *et al.* 2006; Yodzis & Innes 1992) to simulate the dynamics of a range of food webs in space. These models utilize body size and metabolic type to make inferences about parameter values and constrain species to physiologically realistic values. By pairing these models with interaction structures generated by the niche model (Williams & Martinez 2000) we can ensure that each artificially generated food web makes sense ecologically.

Using this allometric modelling framework, we compare the persistence of a range of food webs when isolated and when spatial, particularly describing how differences in the frequency of asynchrony among food webs relate to their persistence when isolated. Following this, we determine the properties of food web structure responsible for the differences in asynchrony and spatial persistence. Finally, we compare the combined effects of both isolated and spatial persistence mechanisms to understand how both sets of mechanisms interact. Surprisingly, we observe an inverse relationship between the ability of food webs to persist when isolated and their tendency to be asynchronous when spatial, limiting the ability of food webs that are persistent when isolated to benefit from spatial persistence mechanisms. As a result, the overall persistence of spatial food webs is determined by a complex interplay between the ability of a given food web to persist when isolated and the action of spatial coexistence mechanisms. This confounds the prediction of a food web's persistence from historically well-studied mechanisms of isolated persistence, with significant implications for ecological theory and conservation planning.

4.2 Methods

To model trophic metacommunity dynamics we use an allometric consumer-resource model (Yodzis & Innes 1992) extended with dispersal and generalized for i

species and p patches:

$$\frac{dB_{i,p}}{dt} = F(B_{i,p}) + G(B_{i,p}) - H(B_{i,p}) - I(B_{i,p}) + J(B_{i,p}) \tag{4.1}$$

$$F(B_{i,p}) = B_{i,p} a_{r,i} M_i^{-.25} (1 - \frac{B_{i,p}}{K_{i,p}}) \tag{4.2}$$

$$G(B_{i,p}) = B_{i,p} a_{x,i} y_i M_i^{-.25} \frac{\sum_{j=1} \omega_{i,j} B_{j,p}^h}{B_0^h + \sum_{j=1} \omega_{i,j} B_{j,p}^h} \tag{4.3}$$

$$H(B_{i,p}) = \sum_{j=1} \frac{B_{j,p} a_{x,j} y_j M_j^{-.25} \omega_{j,i} B_{i,p}^h}{e_{j,i}[B_0^h + \sum_{k=1} \omega_{j,k} B_{k,i}^h]} \tag{4.4}$$

$$I(B_{i,p}) = B_{i,p} a_{x,i} M_i^{-.25} \tag{4.5}$$

$$J(B_{i,p}) = m_i \sum_{q=1} L_{q,p} B_{q,p} \tag{4.6}$$

Here the function F defines the primary production of a producer, G a consumer's growth from consumption, H the biomass lost from predation, I the biomass lost from metabolic processes, and J the net change in a population due to immigration and emigration. All species are either producers or consumers; for producers G and I are set to 0, and likewise F is set to 0 for consumers.

In this model $B_{i,p}$ is the biomass of species i in patch p, M its average body mass, and m its species-specific dispersal rate. For resource species, a_r is its mass-specific growth rate and K its carrying capacity. For consumer species, a_x is its mass-specific metabolic rate, y its maximum consumption rate relative to metabolic rate, $e_{i,j}$ its assimilation rate for species j. The functional response of consumers is defined by B_0, the half-saturation coefficient, and h, the shape parameter. We use a single set of physiological parameters to limit model complexity, $a_x = .88, y = 4, e = .65$. These parameters correspond to a food web of omnivorous vertebrate ectotherms and have been well-studied previously (Brose *et al.* 2006; Lin & Sutherland 2013). We also use a type II functional response, ($B_0 = .5, h = 1$), as the limit cycles a type II functional response is prone to are highly sensitive to the effects of dispersal and emphasize the effects of space on the food web. Finally, units of biomass and time are scaled by the basal resource's growth rate a_r and carrying capacity K respectively. Thus both a_r and K are set to 1 for all patches.

Community interactions

Interactions between species (consumption) are defined by the matrix ω, where each element $\omega_{i,j}$ indicates the relative effort species j spends consuming species i; each column j sums to 1, the total effort each species has to allocate. The interaction matrix ω was generated using the niche model (Williams & Martinez 2000), with relative feeding effort split evenly between all of a predator's available prey. We use the niche model due to both its success in reproducing many of the properties of real food webs and its ease of computation. From the interaction structure each species' trophic level is determined based on the shortest path distance from a basal resource, which is then used to define each species body mass M following the methods of Brose *et al.* 2006, where $M = M_0 \times 10^{ZT}$, M_0 is the mass of the basal resource, Z is the predator-prey body mass ratio, and T the trophic level. We used $Z = 2$, an intermediate value which allows for oscillatory dynamics and many food webs reliant upon spatial persistence mechanisms without being so restrictive as to prevent the coexistence of any species. The mass of the basal resource M_0 affects the time scale of dynamics by influencing growth rate alongside a_r, but has no other effect on dynamics as the ratios of body mass been species are not affected. Thus we set $M_0 = 10^{-1}$. We simulated dynamics for food webs of four to six species, attempting to use all possible food web configurations for these numbers of species by exhaustively sampling the niche model until no additional unique food webs could be readily found. Food webs which included symmetric feeding links (two species feeding on one another) were omitted. All food webs were also constrained to one producer, keeping the total potential energy supply constant among all food webs following the methods of Brose *et al.* 2006. This allowed us to focus on the effects of the structure of interactions rather than differences in the resource base among food webs.

Differences between food web structures are characterized primarily in terms of the number of species, maximum trophic level, and the average consumer-resource body size ratio (CRBSR). Consumer-resource body size ratios, defined as M_j/M_i for each feeding relationship where j feeds on i, has previously been found to play an important

role in determining the dynamics of allometric models (Brose *et al.* 2006). We also found maximum trophic level to be a useful metric for explaining differences among food webs, although this appears to be partially confounded with the effects of average CRBSR: as maximum trophic level increases, food webs become more chain-like with higher average CRBSR. Many other measures were considered and tested, particularly the quantitative food web descriptors from Bersier *et al.* 2002 and information-theoretic indicies from Ulanowicz *et al.* 2009, however these were found to have little to no relationship with differences in food web persistence or asynchrony.

Neither average CRBSR or maximum trophic level alone effectively capture all of the differences we observe in food web dynamics however, thus we devise a new metric which captures the relative strength of high CRBSR food chains within the food web. First we characterize each species in terms of their participation in optimal feeding relationships (where the body size of the consumer is greater than the body size of the resource) using the following metric, ψ:

$$\psi_i = \sum_{j=1} \dot{\omega}_{ji} \psi_j \tag{4.7}$$

where (4.8)

$$\dot{\omega}_{ji} = \begin{cases} \omega_{ji}, \text{for } M_i > M_j \\ 0, \text{for } M_i \leq M_j \end{cases} \tag{4.9}$$

Additionally, ψ is set to 1 for basal resources. The calculation of this metric removes all links where consumers are smaller or equal in size to their resources, and includes each resource's participation in optimal feeding relationships as well. By including the feeding relationships of each consumer's resource, this metric emphasizes chains of optimal feeding relationships, with the maximum value ($\psi_i = 1$) reached only if every interaction in each chain leading back from species i to the basal resource has a CRBSR greater than 1. From ψ, we calculate a CRBSR adjusted trophic level for each species i equal to (Trophic Level $i - 1$)+ψ_i. Species in a linear chain of high CRBSR feeding links will have the same unadjusted and CRBSR adjusted trophic level as ψ_i will equal 1, while

other species will have lower CRBSR adjusted trophic level based on their deviation from the optimal CRBSR. The whole community is then described in terms of the maximum CRBSR adjusted trophic level.

Spatial interactions

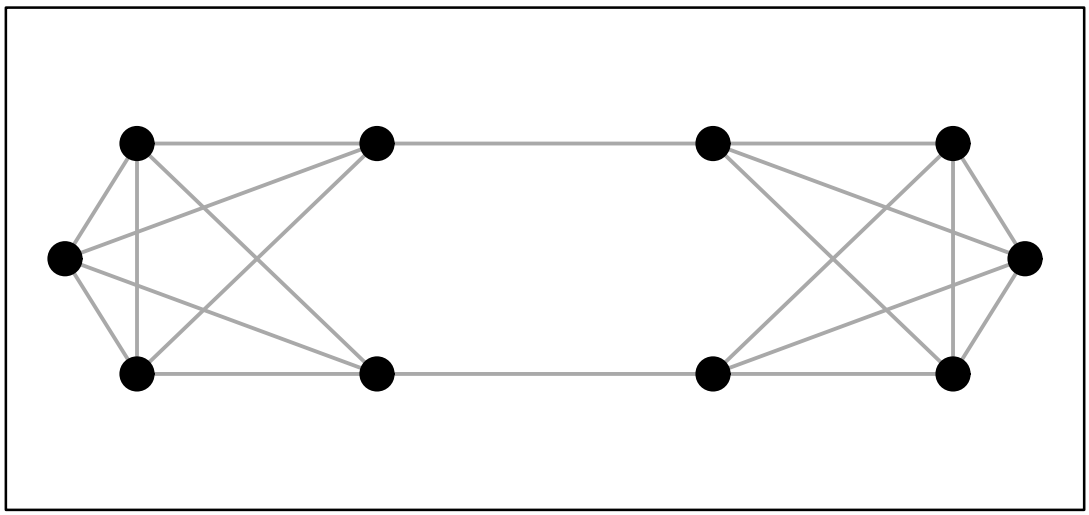

Figure 4.1: Dispersal structure used for all spatial simulations. Each circle represents a patch i which contains a local food web, with each gray line to a neighboring patch j specifying a dispersal connection, or $L_{ij} = L_{ji} = 1$. This structure can be thought of as two symmetrical modules of five patches each, with three interior patches connected to every other patch in the module and two exterior patches which connect to their opposite exterior patch.

Interactions between populations (dispersal) are defined by the matrix L, where each element $L_{q,p}$ indicates the strength of dispersal from patch q to p relative to the species dispersal rate m_i. The diagonal elements $L_{p,p}$ are the negative total of dispersal from patch p ($-L_{p,p} = L_{.,p}$), representing emigration. For our simulations we use a single spatial structure (Fig. 4.1) to remove any confounding effects of variation in spatial structure, focusing only on the effect of variation in food web structure. The spatial structure we used has ten patches, the smallest number we found to be able to readily support asynchrony under the conditions of our simulation. For the specific structure, we

chose a structure in which each patch is linked by dispersal to the same number of other patches. Specifically, each species in each patch can immigrate to and emigrate from four other patches, and dispersal connections are always symmetric such that $L_{p,q} = L_{q,p}$.

We selected the spatial structure used in our simulations for a high tendency toward asynchrony. Synchronous dynamics remove the effect of dispersal as abundances are equal for all patches (or $B_{i,p} = B_{i,j} = B_i$), making the dispersal term $m_i \sum_{q=1} L_{q,p} B_{q,p} = m_i B_i (L_{p,p} + L_{.,p}) = 0$. Thus it is necessary to focus on asynchronous dynamics to observe and compare differences in the response of food webs to spatial dynamics. For the specific structure, we selected the structure with the highest tendency to be asynchronous from the set of all ten-patch 'regular' spatial structures, in which all patches have the same number of neighboring patches to disperse to (in our case, four) (Hayes & Anderson 2017). While many other comparable structures could potentially be used, regular structures constrain the metacommunity such that all communities are functionally identical, avoiding many possible effects idiosyncratic to a single structure caused by introducing differences among communities. Similarly, we set dispersal m to .001 for all species and simulations, an intermediate value for which asynchrony is common but not guaranteed.

Simulation methods

We generated dynamics for each food web under random initial conditions, with each population's starting density chosen uniformly from the interval $[.2, 1.8]$. This range was chosen as a relatively variable set of initial conditions that could produce asynchrony if asynchrony was possible, but within the range of equilibrium abundances observed for most species in our simulations. Simulations lasted for 60000 time steps, as food webs were found to reach equilibrium by 50000, with the remaining 10000 time steps used to measure equilibrium dynamics. This procedure was then replicated 100 times for each spatial food web. The dynamics of each food web were also simulated in the absence of dispersal 1000 times (the number of spatial simulations times the number of patches in spatial simulations) to provide an effective comparison for the effects of space on each

food web's dynamics. Simulations were carried out using the FORTRAN Odepack solver lsoda (Hindmarsh 1983).

Persistence and asynchrony

The ability of species to persist for each simulation was characterized first in terms of feasibility, the requirement that all species can achieve equilibrium without extinction. If a food web reached feasible equilibrium, the minimum regional abundance of each species during equilibrium was measured. These measures describe first whether a food web is capable of supporting the persistence of all species and, among feasible food webs, the extinction risk of each species during equilibrium. As demographic and environmental stochasticity are not included in our model species are never observed to go extinct after reaching a feasible equilibrium, however their minimum abundance provides a strong indication of their risk of extinction when either source of stochasticity is present, as they would be in nature.

As abundances are able to be arbitrarily small and still recover so long as they remain positive in this model, it was necessary to set a non-zero extinction threshold at which point population was considered extinct. We chose $1e^{-10}$; to be feasible, at least one population for each species in the food web must maintain an abundance higher than $1e^{-10}$ at all times. Species minima were measured during equilibrium (the final 10000 time steps of each simulation), specifically the sum of abundances across all patches for each species, the regional total. Species minima were scaled by the number of patches (ten if spatial, one if non-spatial), effectively rescaling abundances such that the patch size of the non-spatial control is equal to the combined size of all patches for the spatial food webs. This enables the values for spatial treatments and non-spatial controls to be compared. Food webs as a whole were characterized in terms of their most vulnerable species, the species with the lowest total regional species minima.

Finally, (a)synchrony in spatial treatments was characterized by comparing the last 20 time steps of each species' abundances. Two patches were considered synchro-

nized if all abundances for all species were within .01 of each other. While this is a strict definition of synchrony, it was found to produce the same results as comparable procedures for determining synchrony in deterministic simulations (Holland & Hastings 2008) while being easier to compute. Asynchronous equilibria were distinguished by the number of synchronized clusters, where each synchronized cluster is a set of synchronized food webs with unique dynamics. For example, an asynchronous equilibrium with ten clusters would have all food webs with unique dynamics, and thus none synchronized, while an equilibrium with two clusters would have two sets of food webs synchronized within each cluster but distinct between clusters.

4.3 Results

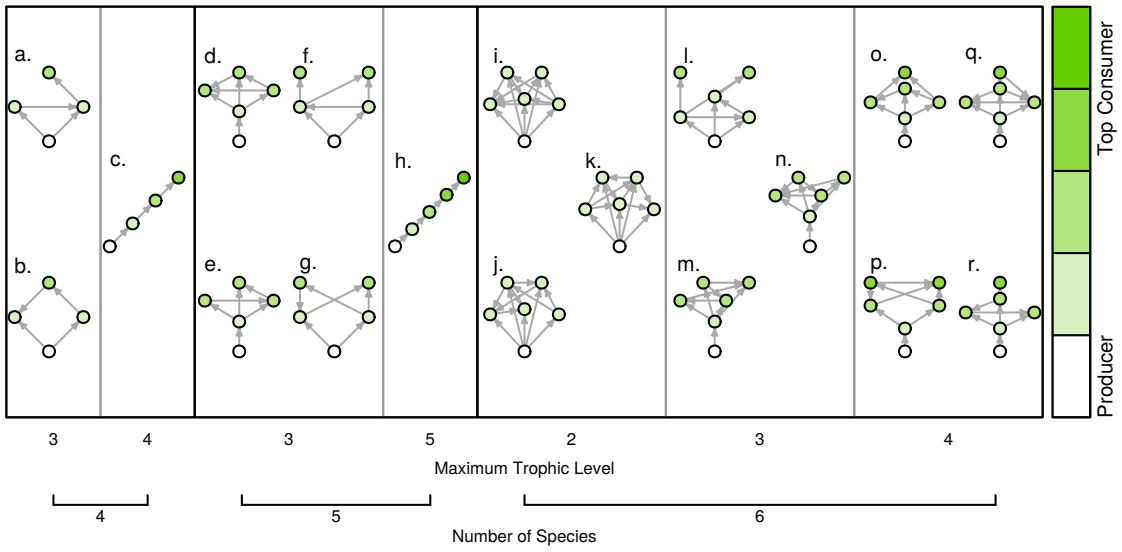

Figure 4.2: Illustration of all food webs which were feasible in at least one simulation. The direction of arrows indicates the flow of energy, such that $s_1 \rightarrow s_2$ indicates that s_1 is eaten by s_2.

Unsurprisingly, the majority of food webs tested were not feasible in either isolated or spatial treatments; only three four-species webs, five five-species webs, and ten

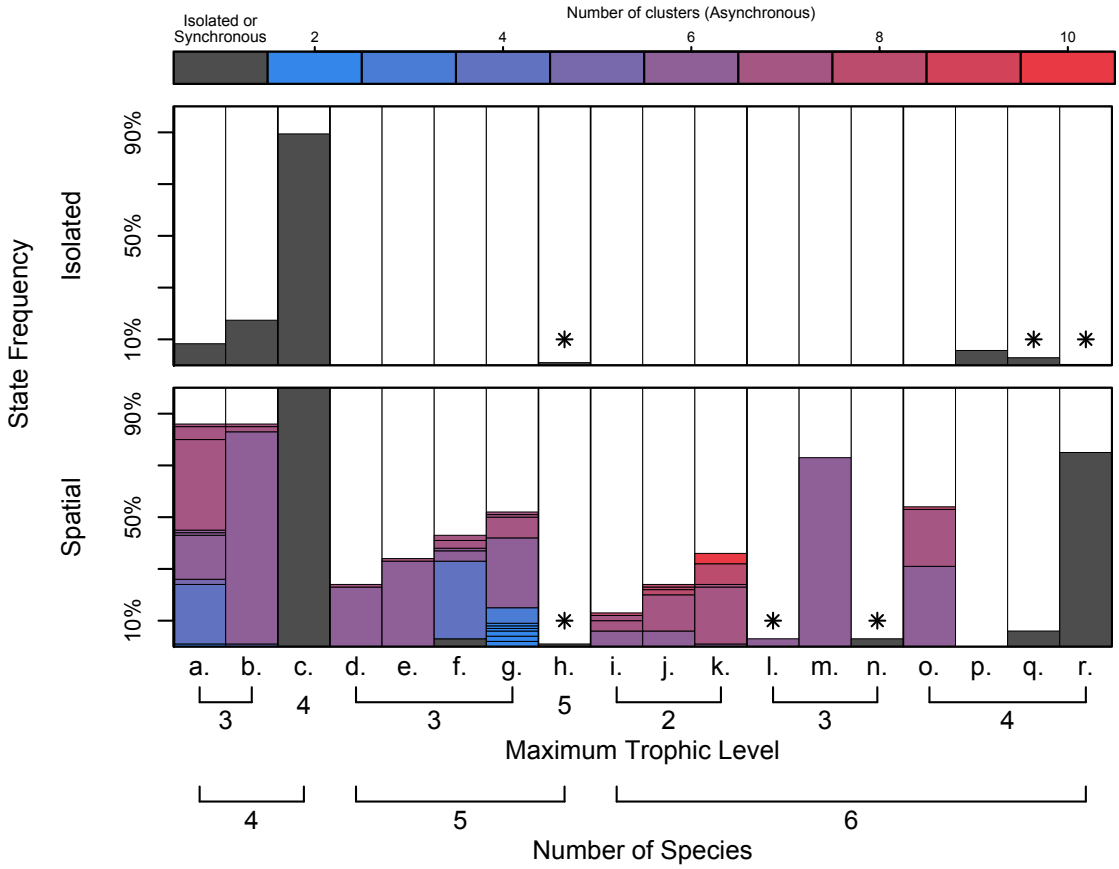

Figure 4.3: Comparison of the frequency of asynchronous states across food webs and relationship with feasibility in isolated treatments. A (*) symbol denotes that a food web is feasible for a given treatment but only rarely, specifically in less than 5% of simulations. Each synchronized cluster is a set of synchronized food webs with unique dynamics, thus number of clusters is the number of unique sets of dynamics present among patches for a given equilibrium. When spatial, many food webs produce stable asynchronous dynamics with multiple patterns of clustering. Food webs which are feasible when isolated rarely exhibit asynchronous dynamics, however.

six-species webs were capable of supporting the coexistence of all original species (Figure 4.2). Following this we characterize the relative ability of each of these food webs to persist, first in terms of their frequency of feasibility in isolated and spatial treatments in Figure 4.3. As expected, food webs are able to reach feasible equilibria more often in spatial treatments, with eleven out of the eighteen food webs only able to persist in the presence of dispersal. What was not expected is that the food webs which are most commonly feasible when isolated appear to receive the least benefit from becoming spatial,

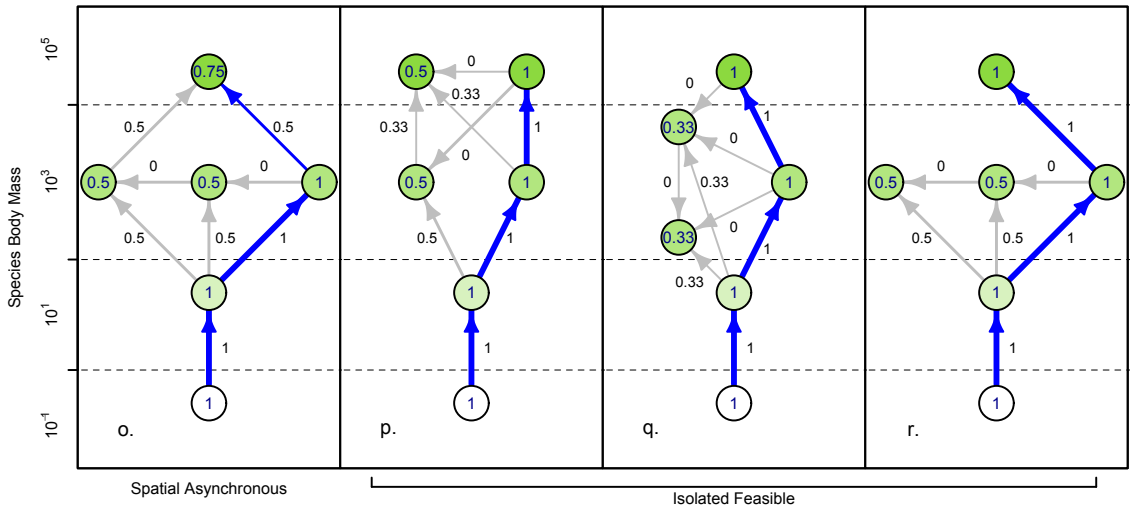

Figure 4.4: Illustration of differences in six species food web structures. Each node represents a species i labeled with its metric for participation in feeding relationships with larger consumers and smaller resources, ψ. Each arrow a feeding interaction such that $i \rightarrow j$ indicates j eats i, labeled with size ratio adjusted interaction strength $\dot{\omega}_{ji}$. The adjusted interaction strength $\dot{\omega}_{ji}$ is 0 if the body size of the resource is equal or greater than the body size of the consumer, and equal to the original interaction strength ω_{ji} otherwise. The interactions highlighted in blue indicate the strongest food chain between a species of the top trophic level and the basal resource. This demonstrates the difference between spatially asynchronous and isolated feasible webs: though the spatially asynchronous food web o. and the spatially synchronous, feasible when isolated food webs p., q., and r. have the same maximum unadjusted trophic level, p., q., and r. each have a strong food chain of made up of interactions with CRBSRs greater than one. By contrast, food web o.'s top species connects a chain with high CRBSRs and chains with low CRBSRs, reducing feasibility when isolated by increasing asynchrony.

remaining synchronous and, with the exception of food web r., changing little in terms of the frequency of feasible equilibria. Conversely, asynchrony is most common in the food webs which are not feasible when isolated.

For the four- and five-species food webs, the frequency of feasibility when isolated and synchrony when spatial is predicted well by high maximum trophic level. For the four-species webs, food web c. is a linear chain with the highest maximum trophic level possible for its size, and is the only food web which is synchronous when spatial, as is the case for food web h. among the five species webs. This pattern does not hold for the six-species webs however. The six-species linear food chain is not feasible, and while the three six-species webs which are feasible in isolation and synchronous when spatial (p.,q.,r.) have the highest maximum trophic level observed among feasible six-species webs (four), one food web (o.) has the same number of trophic levels but is not feasible

Table 4.1: Comparison of measures of food web structure for all feasible webs. While measures of the average consumer-resource body size ratio (CRBSR) and maximum trophic level alone do not predict feasibility when isolated, the combined measure of CRBSR adjusted trophic level does. Specifically, all food webs with a maximum CRBSR adjusted trophic level of 4 or higher is feasible when isolated.

	Species	Average CRBSR	Maximum Trophic Level	Maximum CRBSR Adjusted Trophic Level
Feasible when isolated				
c.	4	10^{2}	4	4.00
h.	5	10^{2}	5	5.00
p.	6	$10^{1.75}$	4	4.00
q.	6	$10^{1.88}$	4	4.00
r.	6	$10^{1.86}$	4	4.00
Asynchronous when spatial and/or not feasible when isolated				
a.	4	$10^{1.88}$	3	2.5
b.	4	$10^{1.88}$	3	3.00
d.	5	$10^{1.76}$	3	3.00
e.	5	$10^{1.83}$	3	3.00
f.	5	$10^{1.92}$	3	2.75
g.	5	$10^{1.92}$	3	3.00
i.	6	$10^{1.56}$	2	2.00
j.	6	$10^{1.63}$	2	2.00
k.	6	$10^{1.59}$	2	2.00
l.	6	$10^{1.88}$	3	3.00
m.	6	$10^{1.75}$	3	3.00
n.	6	$10^{1.70}$	3	3.00
o.	6	$10^{1.88}$	4	3.75

in isolation and asynchronous when spatial.

The differences between these food webs can be captured by considering species consumer-resource body size ratios (CRBSRs) and our CRBSR adjusted maximum trophic level however, as illustrated in Figure 4.4 and Table 4.1. Unlike food webs p., q., and r., the top species of food web o. has feeding relationships split between high and low CRBSR chains, while the top species of the others feed exclusively on a high CRBSR chain.

Following this, all food webs with a maximum CRBSR adjusted trophic level of four or greater is feasible when isolated and synchronous when spatial. Thus chains of feeding relationships between larger consumers and smaller resources increases food web feasibility when isolated, as has been previously demonstrated in allometric models

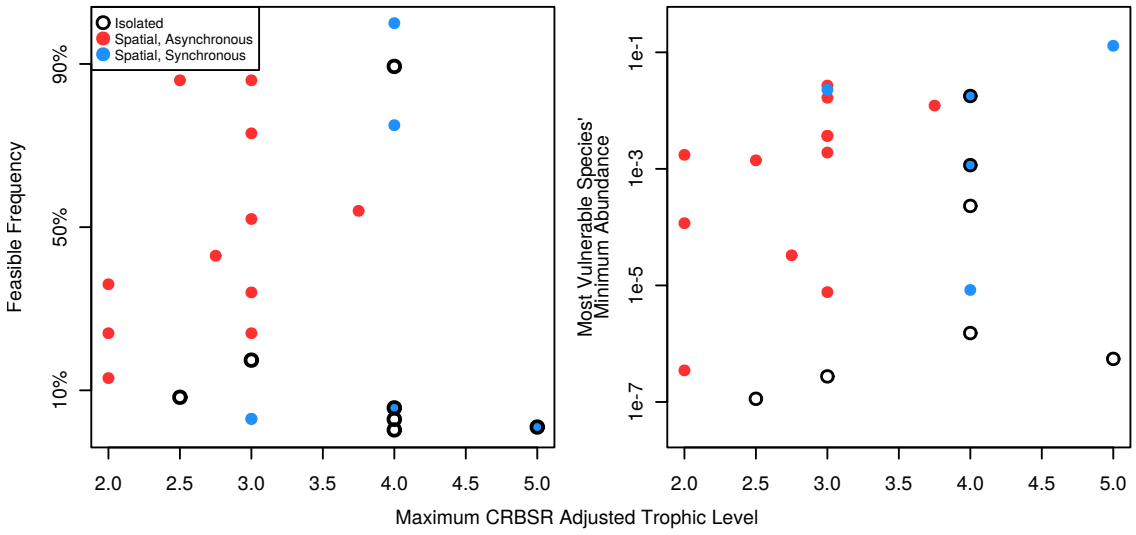

Figure 4.5: Comparison of each feasible food web's maximum CRBSR adjusted trophic level and the minimum abundances of the most vulnerable species. Minimum abundance is calculated from the total abundance of each species across all connected patches, and scaled by the total number of patches to enable comparison between isolated and spatial treatments. The most vulnerable species is the species for each food web with the lowest minimum abundance. These minimum abundances are averaged across all isolated, spatial synchronous, or spatially asynchronous equilibria observed for each food web.

(Brose *et al.* 2006), but reduces the benefit gained from spatial persistence mechanisms by limiting the frequency of asynchrony. In Figure 4.5 we further explore the consequences of this relationship between food web structure and synchrony by illustrating the relationship between maximum CRBSR adjusted trophic level, each food web's ability to reach equilibrium (feasibility) and extinction risk at equilibrium (in terms of the most vulnerable species' minimum abundance). In both cases, a positive relationship between maximum CRBSR adjusted trophic level and feasibility or extinction risk appears when isolated treatments alone are considered. However when spatial treatments are included, this relationship vanishes for feasible frequency and becomes much weaker for minimum abundance. This is due to the negative feedback between asynchrony and feasibility when isolated: the benefits of asynchrony-enabled spatial persistence mechanisms equal or exceed the benefits of high maximum CRBSR adjusted trophic level in many cases.

To complicate matters further, it appears in some cases that spatial dynamics can

enable metacommunities to reach a different synchronous equilibria than found in isolation. Specifically the minimum of food web h., the five-species linear chain (Maximum CRBSR adjusted trophic level = 5), can be seen in Fig. 4.5 to shift from $10^{-6.26}$ when isolated to $10^{-.88}$, despite remaining synchronous in both cases. This is possible when a given food web has multiple alternative isolated equilibria, but one is favored due to an effect of dispersal on the transient dynamics. While this effect plays a role in changing the persistence ability in some food webs, others receive no benefit, creating yet another dimension of variation in the response of differing food web structures to dispersal.

Taken together our results illustrate clearly that differences in food web structure create differences in the frequency of asynchrony, specifically in that asynchrony is uncommon in food webs with long, high CRBSR food chains. This leads to substantial differences in the benefit each food web experiences from spatial coexistence mechanisms. Furthermore, because the same features which reduce the frequency of asynchrony also increase feasibility when isolated, a trade-off between the effect of isolated and spatial persistence mechanisms appears. This trade-off makes the prediction of a food web's persistence when spatial extremely challenging - food webs with high isolated persistence may remain synchronous but exhibit high persistence, while others may switch to high persistence when spatial despite struggling when isolated.

4.4 Discussion

Our results clearly show a general increase in the ability of species within food webs to coexist as a result of the effects of dispersal and asynchrony. Asynchrony in this model differs from what has been commonly discussed in the literature however, in that it is not the result of a spatially heterogeneous environment (Amarasekare & Nisbet 2001; Levin 1976; Mougi & Kondoh 2016) or variation in dispersal ability among species (Amarasekare 2008; McCann *et al.* 2005; Pillai *et al.* 2011); in our model, all patches are identical and dispersal is equal for all species. Rather, the asynchronous equilibria we ob-

serve are alternative stable states that emerge purely from the interactions between food webs via dispersal, a type of self-organizing patterns observed in distributed systems across many fields (Turing 1952). The asynchronous equilibria which result from this pattern formation in ecological systems have been universally shown to reduce fluctuations in population abundances relative to synchronized equilibria (Holland & Hastings 2008; Marleau *et al.* 2014), as they do in our simulations.

While it has been previously demonstrated that the frequency and quality of asynchrony via pattern formation depends strongly on the structure of dispersal within a trophic metacommunity (Hata *et al.* 2014; Holland & Hastings 2008; Marleau *et al.* 2014), our results show that this depends on the structure of interactions within food webs as well. Moreover, the strongest determinant of a trophic metacommunity's ability to form stable asynchronous patterns appears to be the inability to persist in isolation. Considered in terms of pattern formation, this is actually the expected result: the most commonly invoked mechanism for the formation of asynchronous patterns is the destabilization of the synchronized, homogeneous state known as the Turing instability (Turing 1952). Food webs which can persist in isolation are guaranteed to have a stable synchronized equilibrium, as this equilibrium will effectively produce the dynamics of a single large isolated patch. Thus when a food web with a stable synchronous equilibrium is in a spatial environment, any asynchronous equilibria must compete with the synchronous one. The more stable the synchronous equilibrium is, in terms of the tendency of the system to return to it following a perturbation, the less likely it is to escape it and reach an asynchronous equilibria. This is illustrated in the comparison between food webs a. and b. and food web c. in Figure 4.3. Food webs a. and b., which are not often able to return to synchrony following perturbation, switch to asynchronous equilibria when spatial, while food web c., which is almost always able to return to equilibrium without extinction when isolated, remains synchronous when spatial.

The inverse relationship we observe between a food web's ability to persist when isolated and to become asynchronous via pattern formation makes predicting the ability

of food webs to persist in spatial environments challenging. Food webs are not found to be worse at persisting in spatial environments relative to isolated controls, however there is tremendous variation in the degree to which food webs can benefit from the spatial stabilizing mechanisms. Thus while food webs which are feasible in isolation are unable to capitalize on the benefits provided by asynchrony, asynchronous food webs may still be less able to persist depending on the pattern of asynchrony and the food web's interaction structure. Rather the ultimate ability of a food web to persist depends on a complex interaction between its ability to persist locally and to exploit the coexistence mechanisms provided by spatial environments.

Following this, the prediction of food web persistence becomes significantly more challenging. In our simulations we observe that the maximum CRBSR adjusted trophic level, a measure of structure emphasizes strong chains of interactions between species with high consumer-resource body size ratios, is a good predictor of persistence in isolated food webs. This agrees with previous results investigating the persistence ability of isolated food webs, which find that the high ratios of consumer-resource body sizes play a critical role in species persistence for isolated communities (Brose *et al.* 2006). The results of our spatial simulations complicate the relationship between body size and persistence however. When spatial, food webs with lower maximum CRBSR adjusted trophic level, indicating a weaker backbone of strong, high CRBSR interactions, often have a comparable if not better ability to maintain species persistence relative to those with higher maximum CRBSR adjusted trophic levels. Other examples of context-dependent effects of food web properties have been noted previously when comparing the effects of food web properties across a gradient of dispersal strength, particularly the number of species (Plitzko & Drossel 2015) and weak trophic interactions (Maser *et al.* 2007). Our work builds upon these observations by specifically demonstrating that these context-dependent effects of food web properties can result due to unexpected effects of local food web dynamics and the structural properties that drive them on the potential for food webs to achieve asynchrony.

Our findings may also have important implications for conservation. Top predators are disproportionately threatened by human development while being known to play important roles in the functioning of many communities (Heithaus *et al.* 2008; Ripple *et al.* 2014). In the context of our results, top predators play a cental role role in extending the high CRBSR chains which are the key to the persistence of isolated food webs. The ability of food webs with fewer trophic levels to improve persistence when spatial, then, represents a possible approach for maintaining species persistence for food webs with threatened top predators. Following the loss of a top predator's stabilizing influence, species persistence may be preserved by changing to an alternative asynchronous regime. This emphasizes the importance of maintaining spatial connectivity among food webs, and restoring it where it is lost. As the underlying mechanisms of pattern formation suggest that any loss in stability of the synchronized or isolated equilibrium translates into a greater ability to become asynchronous, the shift from isolated to spatial persistence mechanisms may be useful in buffering the affects of not only the loss of top predators, but many other threats as well.

Altogether our findings strongly suggest that a food web's persistence when isolated cannot readily predict its persistence in a spatial environment. There appears to be an additional but relatively unexplored layer of food web properties which determine the ability of a food web to capitalize on the stabilizing opportunities created by dispersal with neighboring patches, specifically the tendency to become asynchronous. More investigation is needed to generalize these findings beyond the specific cases we explore however, particularly in that pattern formation is the only mechanism capable of producing asynchrony in our simulations. Further study expanding these results to include the effects of spatially heterogeneous environments and variation in the ability of species to disperse on the ability of food webs to achieve asynchrony in particular is important moving forward. Nevertheless, our results represent an important step forward by shedding light on the role of asynchronous pattern formation in determining the persistence of food webs in space. Given the ubiquity of dispersal in real food webs and the rapid

alteration of the spatial environment due to human activity, it is more important than ever to understand the role of spatial dynamics in enabling the persistence of species underlying the great diversity we observe in nature.

Bibliography

Amarasekare, P. (2008). Spatial dynamics of foodwebs. *Annual Review of Ecology, Evolution, and Systematics*, 39, 479–500.

Amarasekare, P. & Nisbet, R. M. (2001). Spatial heterogeneity, source-sink dynamics, and the local coexistence of competing species. *The American Naturalist*, 158, 572–584.

Bersier, L.-F., Banašek-Richter, C. & Cattin, M.-F. (2002). Quantitative descriptors of food-web matrices. *Ecology*, 83, 2394–2407.

Briggs, C. J. & Hoopes, M. F. (2004). Stabilizing effects in spatial parasitoid–host and predator–prey models: a review. *Theoretical population biology*, 65, 299–315.

Brose, U., Williams, R. J. & Martinez, N. D. (2006). Allometric scaling enhances stability in complex food webs. *Ecology Letters*, 9, 1228–1236.

Brown, J. H. & Kodric-Brown, A. (1977). Turnover rates in insular biogeography: effect of immigration on extinction. *Ecology*, 58, 445–449.

Buckling, A., Kassen, R., Bell, G. & Rainey, P. B. (2000). Disturbance and diversity in experimental microcosms. *Nature*, 408, 961–964.

Chesson, P. & Huntly, N. (1997). The roles of harsh and fluctuating conditions in the dynamics of ecological communities. *The American Naturalist*, 150, 519–553.

Gouhier, T. C., Guichard, F. & Gonzalez, A. (2010). Synchrony and stability of food webs in metacommunities. *The American Naturalist*, 175, E16–E34.

Hata, S., Nakao, H. & Mikhailov, A. S. (2014). Dispersal-induced destabilization of metapopulations and oscillatory Turing patterns in ecological networks. *Scientific Reports*, 4.

Hayes, S. M. & Anderson, K. E. (2017). Beyond connectivity: how the structure of dispersal influences metacommunity dynamics. Manuscript.

Heithaus, M. R., Frid, A., Wirsing, A. J. & Worm, B. (2008). Predicting ecological consequences of marine top predator declines. *Trends in Ecology & Evolution*, 23, 202–210.

Hindmarsh, A. C. (1983). ODEPACK, A Systematized Collection of ODE Solvers, RS Stepleman et al.(eds.), North-Holland, Amsterdam,(vol. 1 of), pp. 55-64. *IMACS Transactions on Scientific Computation*, 1, 55–64.

Holland, M. D. & Hastings, A. (2008). Strong effect of dispersal network structure on ecological dynamics. *Nature*, 456, 792–794.

Kartascheff, B., Heckmann, L., Drossel, B. & Guill, C. (2010). Why allometric scaling enhances stability in food web models. *Theoretical Ecology*, 3, 195–208.

Leibold, M. A., Holyoak, M., Mouquet, N., Amarasekare, P., Chase, J., Hoopes, M., *et al.* (2004). The metacommunity concept: a framework for multi-scale community ecology. *Ecology Letters*, 7, 601–613.

Levin, S. A. (1976). Population dynamic models in heterogeneous environments. *Annual Review of Ecology and Systematics*, 7, 287–310.

Lin, Y. & Sutherland, W. J. (2013). Color and degree of interspecific synchrony of environmental noise affect the variability of complex ecological networks. *Ecological Modelling*, 263, 162–173.

Marleau, J. N., Guichard, F. & Loreau, M. (2014). Meta-ecosystem dynamics and functioning on finite spatial networks. *Proceedings of the Royal Society of London B: Biological Sciences*, 281, 20132094.

Maser, G. L., Guichard, F. & McCann, K. S. (2007). Weak trophic interactions and the balance of enriched metacommunities. *Journal of Theoretical Biology*, 247, 337–345.

May, R. M. (1972). Will a large complex system be stable? *Nature*, 238, 413–414.

McCann, K. S., Rasmussen, J. & Umbanhowar, J. (2005). The dynamics of spatially coupled food webs. *Ecology Letters*, 8, 513–523.

Mougi, A. & Kondoh, M. (2016). Food-web complexity, meta-community complexity and community stability. *Scientific Reports*, 6.

Pillai, P., Gonzalez, A. & Loreau, M. (2011). Metacommunity theory explains the emergence of food web complexity. *Proceedings of the National Academy of Sciences*, 108, 19293–19298.

Plitzko, S. J. & Drossel, B. (2015). The effect of dispersal between patches on the stability of large trophic food webs. *Theoretical Ecology*, 8, 233–244.

Ripple, W. J., Estes, J. A., Beschta, R. L., Wilmers, C. C., Ritchie, E. G., Hebblewhite, M., *et al.* (2014). Status and ecological effects of the world's largest carnivores. *Science*, 343, 1241484.

Steiner, C. F., Stockwell, R. D., Kalaimani, V. & Aqel, Z. (2011). Dispersal promotes compensatory dynamics and stability in forced metacommunities. *The American Naturalist*, 178, 159–170.

Turing, A. M. (1952). The chemical basis of morphogenesis. *Philosophical Transactions of the Royal Society of London B: Biological Sciences*, 237, 37–72.

Ulanowicz, R. E., Goerner, S. J., Lietaer, B. & Gomez, R. (2009). Quantifying sustainability: resilience, efficiency and the return of information theory. *Ecological Complexity*, 6, 27–36.

Williams, R. J. & Martinez, N. D. (2000). Simple rules yield complex food webs. *Nature*, 404, 180–183.

Yodzis, P. & Innes, S. (1992). Body size and consumer-resource dynamics. *The American Naturalist*, 1151–1175.

Chapter 5

Conclusions

Overall, the work presented here provides a deeper look into the effects and mechanics of maintaining asynchrony between dispersal-linked communities. In particular, we illustrate the role of asynchronous pattern formation between identical patches, an important mechanism which may supplement and confound the effects of environmental heterogeneity on asynchrony in nature. Through a more detailed understanding of the role of pattern formation in maintaining asynchrony in metacommunities, we enable greater insight into the mechanisms which determine how spatial processes influence metacommunities and may be used to enhance community persistence.

First, we focus on the mechanisms by which spatial structure influence maintenance of asynchrony via pattern formation, specifically the properties of spatial structure which determine the frequency of asynchrony. In **Chapter 2**, we demonstrate that differences in the effect of spatial structure between metacommunities appear even among spatial structure with identical connectivity, in terms of both the total amount and distribution of dispersal among patches. These differences are most effectively characterized by the eigenvalues of the dispersal matrix, which describe the relative stability of synchrony among patches in a metacommunity. As increasing stability of the synchronous state has a negative relationship with the frequency of asynchrony, this becomes an effective predictor of the tendency of a spatial structure to maintain asynchrony and the

beneficial effects of dispersal on community dynamics.

From this work we also note a substantial amount of surprising variation among asynchronous metacommunities. In addition to influencing the frequency of asynchrony, variation in spatial structure also dictates the type of asynchronous pattern experienced. These differences in asynchronous dynamics could not be predicted based on the stability of the synchronized state, the common approach for predicting asynchrony in both ecology and the broader fields of complex systems (Arenas *et al.* 2008; Marleau *et al.* 2014; Yeakel *et al.* 2014).

To further investigate this variation in asynchronous dynamics, in **Chapter 3** we devise and analyze a model to predict asynchronous patterns from spatial structure and identify the mechanisms by which structure influences the dynamics of asynchrony. Through this analysis we show several mechanisms by which differences in phase and amplitude are stabilized within systems of identical oscillating subcomponents, including ecological communities.

Moreover, we find that the mechanisms underlying pattern formation in this model generalize readily to more complex ecological dynamics, making the model an effective tool for predicting the effect of spatial structure on the dynamics of asynchronous metacommunities. Differences do emerge in certain cases however, specifically as a result of the nonlinearity of local interactions in the ecological model used. While the model can be adjusted to account for these differences, the resulting complexity presents many challenges.

Following these results, in **Chapter 4** we work to further investigate how local interactions influence asynchrony, particularly how differences in food web structure influence the abilities of metacommunities to maintain asynchrony. While most simulated communities are unable to persist, among those that do we find substantial differences in their tendency to maintain asynchrony which appears to be predicted most strongly by an inability to persist as in an isolated community. This relates back to a common mechanism for pattern formation, the Turing instability, wherein the loss of stability of a

synchronized state promotes asynchrony (Turing 1952). In both the cases of the Turing instability and our simulated communities, asynchrony is promoted by destabilization of the synchronous equilibrium. The results of our simulations differ, however, in that the synchronous equilibrium is destabilized due to local interactions, rather than due to dispersal as in the case of a true Turing instability.

This leads to a complex interaction between the effects of food web structural properties expected from studies of isolated communities and their effects on spatial communities. For example, earlier results using the model we tested found that high ratios between consumer and resource body mass increased the ability of isolated communities to persist. Our simulations produced similar results for isolated communities, but also found that as a result communities with higher consumer-resource body mass ratios were less likely to experience asynchrony. Considering importance of maintaining asynchrony for the action of many spatial persistence mechanisms, it thus becomes challenging to predict the ultimate effect of food web structural properties on a metacommunity. Our results show a range of persistence ability for both synchronous and asynchronous metacommunities, with the effects of both asynchrony and food web structure playing an important role in determining the persistence ability of each metacommunity.

The results of this work suggest several important directions for future study. In particular, the role of local dynamics in promoting or inhibiting asynchrony is not well understood and requires a great deal more study. While our work sheds some light on the role of local interactions in predicting the frequency of synchrony, it is also necessary to investigate how differences in local interactions alter the quality of asynchronous dynamics. Furthermore, the studies presented here focus exclusively on the case of identical communities to better understand pattern formation; to expand on this work it now becomes necessary to consider how the maintenance of asynchrony via pattern formation and environmental heterogeneity interact. The realism of the models considered can also be improved upon, particularly by including differences in dispersal ability among species.

Bibliography

Arenas, A., Dıaz-Guilera, A., Kurths, J., Moreno, Y. & Zhou, C. (2008). Synchronization in complex networks. *Physics Reports*, 469, 93–153.

Marleau, J. N., Guichard, F. & Loreau, M. (2014). Meta-ecosystem dynamics and functioning on finite spatial networks. *Proceedings of the Royal Society of London B: Biological Sciences*, 281, 20132094.

Turing, A. M. (1952). The chemical basis of morphogenesis. *Philosophical Transactions of the Royal Society of London B: Biological Sciences*, 237, 37–72.

Yeakel, J., Moore, J., Guimarães, P. & Aguiar, M. (2014). Synchronisation and stability in river metapopulation networks. *Ecology Letters*, 17, 273–283.